and the macrocycle is C(16)···C(b4) = 3.846 (5) Å; all other distances are larger. Thus the bridging alkyl chains of isomers II and III are not expected to interfere significantly with the binding of axial ligands, although they may interfere with free rotation of bound axial ligands about the M-L bond. Preliminary NMR investigations of low-spin Fe(III) complexes of hexyl II and III with N-MeIm suggest that this is the case, as will be discussed fully in a later publication.

Acknowledgments. The financial support of the National Institutes of Health [Grants AM 31038 (F.A.W.) and HL 15627 (W.R.S.)] is gratefully acknowledged. This work has also been supported by a NATO grant for scientific investigation, administered by the DAAD, West Germany (U.S.), and by a NATO grant for scientific investigation, administered by GNAM-OTAN, France (B.J.H.). B.J.H. also acknowledges receipt of a research leave from the University of Dijon. The Department of Chemistry, San Francisco State University, also acknowledges grants from the National Institutes of Health (RR 02684) and the National Science Foundation (DMB-8516065) for purchase of the NMR spectrometers. Some NMR spectra were recorded on the Nicolet NT-360 at the University of California, Davis, NMR facility, and on the Bruker WM-500 at the University of California, Berkeley. X-ray crystal structure analyses were performed at the University of Notre Dame. The authors also thank Dr. Charles W. Eigenbrot for collecting the data set for Zn hexyl II.

Supplementary Material Available: Tables of anisotropic thermal parameters, fractional coordinates, and isotropic thermal parameters (2 pages); listing of observed and calculated structure factors (13 pages). Ordering Information is given on any current masthead page.

Dioxygen-Copper Reactivity. Reversible Binding of O_2 and CO to a Phenoxo-Bridged Dicopper(I) Complex

Kenneth D. Karlin,* Richard W. Cruse, Yilma Gultneh, Amjad Farooq, Jon C. Hayes, and Jon Zubieta

Contribution from the Department of Chemistry, State University of New York at Albany, Albany, New York 12222. *Received September 24, 1986*

Abstract: A chemical system possessing features that mimic certain structural properties and the O_2 binding behavior of the active site of the copper-containing dioxygen carrier hemocyanin (Hc) is presented. A phenolic dinucleating ligand possessing two tridentate py2 units (py2 = bis(2-(2-pyridyl)ethyl)amine) (XYL-OH) forms a phenoxo-bridged dicopper(I) complex, $[Cu_2(XYL\text{-}O\text{-})]PF_6$ (**1**). At −80 °C in dichloromethane solution, **1** reacts with O_2 ($Cu:O_2$ = 2:1) to give an intensely purple-colored dioxygen adduct, $[Cu_2(XYL\text{-}O\text{-})(O_2)]PF_6$ (**2**), having charge-transfer absorptions in the visible region at 505 (ϵ 6000) and 610 (sh) nm (ϵ 2100 $(M\cdot cm)^{-1}$) with additional features at 385 (ϵ 2900), 790 (ϵ 700), and 925 nm (ϵ 600 $(M\cdot cm)^{-1}$). The binding of O_2 to **1** is reversible, and the O_2 ligand can be removed in vacuo to regenerate **1**. This *vacuum cycling* can be followed spectrophotometrically over several cycles. Carbon monoxide and triphenylphosphine react with **1** to form the bis adducts **3**, $[Cu_2(XYL\text{-}O\text{-})(CO)_2]PF_6$ (**3a**) and $[Cu_2(XYL\text{-}O\text{-})(PPh_3)_2]PF_6$ (**3b**), respectively; the reaction with carbon monoxide is also reversible. The dioxygen adduct **2** reacts with CO and/or PPh_3, displacing the bound O_2 ligand and producing the adducts **3**; this behavior further substantiates that the reaction of **1** with O_2 is an equilibrium process. *Carbonyl cycling*, where **1** reacts with O_2 to produce **2**, O_2 is displaced by CO to produce **3a**, and **3a** is decarbonylated to regenerate **1**, can also be followed spectrophotometrically over several cycles. In both cycling procedures, a decomposition product is observed and identified as the phenoxo and hydroxo doubly bridged dicopper(II) complex $[Cu_2(XYL\text{-}O)(OH)]^{2+}$. Crystallographic studies have been completed for both **1** and **3b**. **1** crystallizes in the monoclinic space group $P2_1/n$ with Z = 8 (2 per asymmetric unit) and a = 13.861 (4) Å, b = 13.482 (8) Å, c = 16.956 (5) Å, and β = 98.20 (2)°. Complex **3b** crystallizes in the triclinic space group $P\bar{1}$ with Z = 2 and a = 13.410 (3) Å, b = 14.867 (3) Å, c = 18.990 (4) Å, α = 102.35 (2)°, β = 91.71 (2)°, and γ = 98.68 (2)°. While **1** contains two phenoxo-bridged tetracoordinate Cu(I) ions (Cu···Cu = 3.62-3.72 Å) where each copper atom is also coordinated to the py2 tridentate group, in **3b** one pyridine donor from each py2 unit remains uncoordinated such that each Cu(I) atom is bound by two nitrogen donors, the P atom from a PPh_3 ligand, and the bridging phenoxo oxygen atom (Cu···Cu = 3.992 Å).

The interest in understanding the binding, interaction, and subsequent reactivity of dioxygen (O_2) at copper ion centers stems in part from the occurrence of copper-containing enzymes such as hemocyanin (Hc),[1-5] which transports O_2, and the monooxygenases tyrosinase[1,2b,4-6] and dopamine β-hydroxylase,[1,2b,4-7] which incorporate oxygen (from O_2) into organic substrates. Studies of biomimetic chemical models can be useful in determining the relevant and/or possible coordination chemistry in the proteins and thus help to elucidate structural and spectroscopic properties of the enzyme active sites.[4,5,8] Concepts derived from such studies may also be expected to contribute to the development of practical synthetic systems for the reversible binding of O_2

(1) (a) Solomon, E. I. In *Metal Ions in Biology*; Spiro, T. G., Ed.; Wiley-Interscience: New York, 1981; Vol. 3, pp 41-108. (b) Solomon, E. I.; Penfield, K. W.; Wilcox, D. E. *Struct. Bonding (Berlin)* **1983**, *53*, 1-57.
(2) (a) Lontie, R.; Witters, R. *Met. Ions Biol. Syst.* **1981**, *13*, 229-258. (b) Lerch, K. *Ibid.* **1981**, *13*, 143-186.
(3) Solomon, E. I. In *Copper Coordination Chemistry: Biochemical & Inorganic Perspectives*, Karlin, K. D., Zubieta, J., Eds.; Adenine: Guilderland, NY, 1983; pp 1-22.
(4) Karlin, K. D.; Gultneh, Y. *J. Chem. Educ.* **1985**, *62*, 983-990 and references cited therein.
(5) Karlin, K. D.; Gultneh, Y. *Prog. Inorg. Chem.*, in press.
(6) Robb, D. A. In *Copper Proteins and Copper Enzymes*; Lontie, R., Ed.; CRC: Boca Raton, FL, 1984; Vol. 2, pp 207-241.
(7) Villafranca, J. J. In *Metal Ions in Biology*; Spiro, T. G., Ed.; Wiley-Interscience: New York, 1981; Vol. 3, pp 263-290.
(8) Sheldon, R. A.; Kochi, J. K. *Metal-Catalyzed Oxidations of Organic Compounds*; Academic: New York, 1981.

0002-7863/87/1509-2668$01.50/0

and/or the oxidation of organic compounds.[8]

Extensive chemical, spectroscopic, and X-ray structural studies have contributed to a fairly detailed picture of the active site of the dioxygen-carrying proteins in arthropod and mollusc hemocyanins. Earlier studies had suggested two or three imidazole ligands from histidine as coordinating to the Cu(I) ions at a dinuclear metal center in deoxy-Hc. The recent X-ray structure on the spiny lobster Hc *Panulirus interruptus* shows that the two cuprous ions in this deoxy-Hc are each coordinated to three imidazole nitrogen ligands in a hydrophobic environment, with Cu···Cu = 3.8 ± 0.4 Å.[9] The reaction with O_2 occurs via an

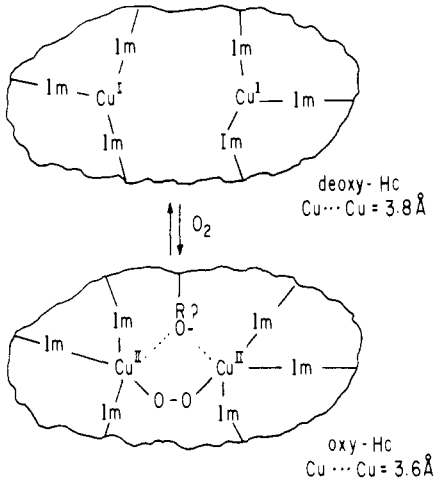

inner-sphere redox process to give oxy-Hc containing a dinuclear Cu(II) center and a coordinated peroxo (O_2^{2-}) ligand. Extensive chemical investigations as well as spectroscopic considerations suggest that each copper(II) ion is found in a tetragonal coordination environment with ligation to either four or five donors including a cis μ-1,2-peroxo moiety. Consistent with these hypotheses are the results from extended X-ray absorption fine structure (EXAFS) measurements that indicate a Cu···Cu separation of ca. 3.6 Å.[10] The presence of an endogenous bridging ligand in oxy-Hc has been proposed[11] on the basis of the observations that (a) oxy-Hc as well as oxidized dicopper(II) derivative forms ("met" and "dimer") of Hc are strongly magnetically superexchange coupled and (b) there is an otherwise unassigned absorption band at 425 nm for oxy-Hc[12] that can be characteristic of phenoxo-bridged dicopper(II) complexes.[1b,11] However, the presence of a protein-derived bridging ligand (e.g., endogenous tyrosine or serine) is not supported by the results of the recent X-ray structural analysis,[9] such that if there is a bridging ligand (other than O_2^{2-}) at all, hydroxide or water seems to be the only likely candidate.

The use of dinucleating ligands containing alkoxo or phenoxo groups (RO^-) has become very popular in biomimetic studies[4,13-15]

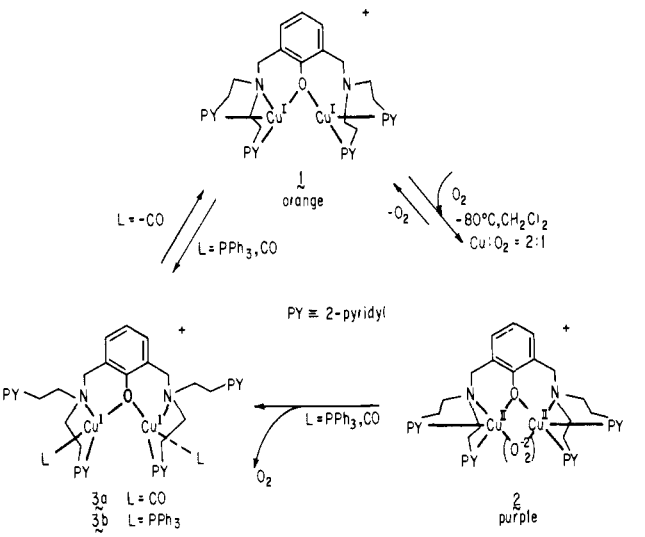

Figure 1. Scheme showing the reactions of the phenoxo-bridged dicopper(I) complex **1** with O_2, CO, and PPh_3. **1** reacts reversibly with O_2 at low temperature in dichloromethane to give the dioxygen adduct **2**, which is best described as a peroxo–dicopper(II) compound. Complex **1** reacts with CO reversibly to give **3a** or with triphenylphosphine to give the bis-adduct **3b**. Carbon monoxide and PPh_3 also react with **2** to give the same adduct complexes **3**, displacing O_2 in the process. The occurrence of the latter reactions further substantiates the reversible (equilibrium) nature of the binding of O_2 to **1**; the reaction of **2** with CO or PPh_3 shifts the equilibrium $\mathbf{1} + O_2 \rightleftharpoons \mathbf{2}$ to the left since **1** reacts with these molecules to produce the adducts **3**. See text for further discussion.

of copper proteins due to (a) the suggestion of their presence in oxy-Hc[1-3,11] and (b) the ease of formation of dinuclear copper complexes using such systems. We recently reported that a tetracoordinate phenoxo-bridged dicopper(I) compound, $[Cu_2(XYL\text{-}O\text{-})]^+$ (**1**), reacts at low temperature in CH_2Cl_2 solution with 1 equiv of dioxygen (O_2) to give an intensely purple-colored dioxygen adduct, $[Cu_2(XYL\text{-}O\text{-})(O_2)]^+$ (**2**) (Figure 1).[16] Complex **2** can be described as a peroxo–dicopper(II) complex on the basis of the observation that in its resonance Raman spectrum it exhibits an absorption at 803 cm^{-1}, assignable to the O–O stretch of a coordinated peroxo (O_2^{2-}) unit.[16] The binding of O_2 to **1** is reversible and cycling between **1** and **2** is possible and can be followed spectrophotometrically. The dicopper(I) complex **1** also forms bis-adducts with the typical Cu(I) specific ligands carbon monoxide (CO) and triphenylphosphine (PPh_3) giving **3a** and **3b** respectively (Figure 1). We find that these adducts, $[Cu_2(XYL\text{-}O\text{-})(L)_2]^+$ (**3**), also form by the displacement of O_2 when the dioxygen complex **2** is directly reacted with either CO or PPh_3. These observations lend further support to the existence of the reversible equilibrium $\mathbf{1} \rightleftharpoons \mathbf{2}$. The reaction of **2** with CO or PPh_3 shifts the equilibrium toward the dicopper(I) species **1** due to the ensuing reaction of **1** to give the adducts **3**; O_2 is liberated in the process. In this paper, we describe the syntheses and properties of compounds **1**, **2**, and **3**, including the reactions of **1** and **2** with O_2, CO, and PPh_3, and we report full X-ray structural studies of complexes **1** and **3b**. We also provide UV–vis spectral evidence for the reversible O_2 and CO binding properties of **1**, i.e., the cycling between **1** and **2** by removal of O_2 under vacuum from **2** (*vacuum cycling*) or the cycling of **1** and **2** via the carbonyl adduct **3a** (*carbonyl cycling*) (see Figure 1).

Results and Discussion

$[Cu_2(XYL\text{-}O\text{-})]^+$ (1). The dinucleating ligand used in compounds **1–3** is the deprotonated form of the phenol IV; IV is produced by a copper-mediated hydroxylation of a dinucleating ligand, *m*-XYLpy2 (py2 = the tridentate group bis(2-(2-

(9) (a) Gaykema, W. P. J.; Hol, W. G. J.; Vereijken, J. M.; Soeter, N. M.; Bak, H. J.; Beintema, J. J. *Nature (London)* **1984**, *309*, 23–29. (b) Linzen, B.; Soeter, N. M.; Riggs, A. F.; Schneider, H.-J.; Schartau, W.; Moore, M. D.; Yokota, E.; Behrens, P. Q.; Nakashima, H.; Takagi, T.; Nemoto, T.; Vereijken, J. M.; Bak, H. J.; Beintema, J. J.; Volbeda, A.; Gaykema, W. P. J.; Hol, W. G. J. *Science (Washington, D.C.)* **1985**, *229*, 519–524. (c) Gaykema, W. P. J.; Volbeda, A.; Hol, W. G. J. *J. Mol. Biol.* **1985**, *187*, 255–275.

(10) (a) Co, M. S.; Hodgson, K. O.; Eccles, T. K.; Lontie, R. *J. Am.Chem. Soc.* **1981**, *103*, 984–986. (b) Co, M. S.; Hodgson, K. O. *Ibid.* **1981**, *103*, 3200–3201. (c) Brown, J. M.; Powers, L.; Kincaid, B.; Larrabee, J. A.; Spiro, T. G. *Ibid.* **1980**, *102*, 4210–4216. (d) Spiro, T. G.; Wollery, G. L.; Brown, J. M.; Powers, L.; Winkler, M. E.; Solomon, E. I. In *Copper Coordination Chemistry; Biochemical & Inorganic Perspectives*; Karlin, K. D., Zubieta, J., Eds.; Adenine: Guilderland, NY, 1983; pp 23–42.

(11) Wilcox, D. E.; Long, J. R.; Solomon, E. I. *J. Am. Chem. Soc.* **1984**, *106*, 2196–2194 and references cited therein.

(12) Kino, J.; Suzuki, S.; Mori, W.; Nakahar, A. *Inorg. Chim. Acta* **1981**, *56*, L33–L34.

(13) *Copper Coordination Chemistry: Biochemical & Inorganic Perspectives*; Karlin, K. D., Zubieta, J., Eds.; Adenine: Guilderland, NY, 1983.

(14) *Biological & Inorganic Copper Chemistry*; Karlin, K. D., Zubieta, J., Eds.; Adenine: Guilderland, NY, 1986; Vol. 2.

(15) McKee, V.; Zvagulis, M.; Dagdigian, J. V.; Patch, M. G.; Reed, C. A. *J. Am. Chem. Soc.* **1984**, *106*, 4765–4772.

(16) Karlin, K. D.; Cruse, R. W.; Gulneh, Y.; Hayes, J. C.; Zubieta, J. *J. Am. Chem. Soc.* **1984**, *106*, 3372–3374.

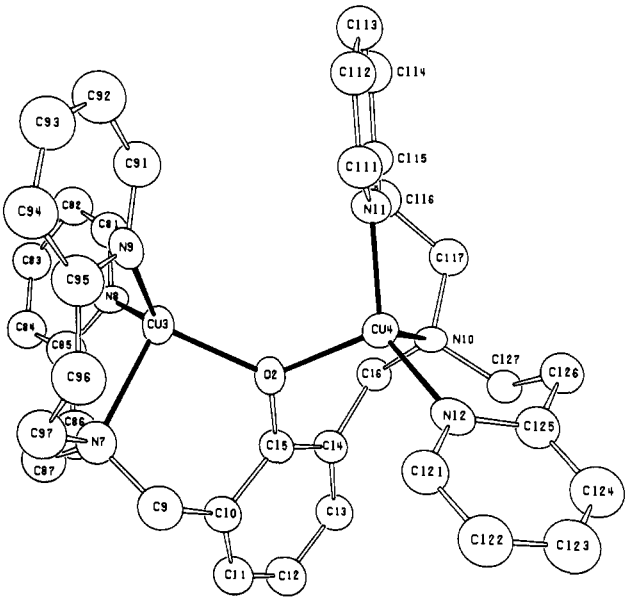

Figure 2. ORTEP diagram of the cationic portion of the phenoxo-bridged dicopper(I) complex **1** showing the atom labeling scheme.

pyridyl)ethyl)amine). The three-coordinate dicopper(I) complex II, containing the ligand I, reacts with dioxygen resulting in the oxygenation of the ligand and the concomitant formation of the phenoxo and hydroxo doubly bridged dinuclear Cu(II) complex III.[17] The free phenol IV can be isolated from III by leaching out the Cu(II) ions using aqueous ammonia followed by extraction of IV with dichloromethane.

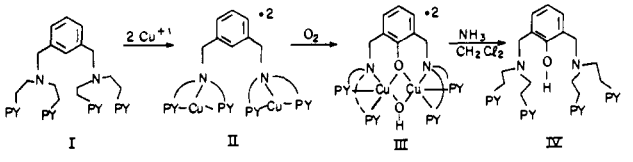

The orange-brown crystals of **1** are formed in high yield by the addition of $Cu(CH_3CN)_4^+$ to IV in methanol in the presence of base. Complex **1**, usually formed as the monocationic hexafluorophosphate (PF_6^-) salt, is stable and soluble in a variety of polar organic solvents such as methanol, acetonitrile, acetone, dichloromethane, and dimethylformamide. While it is stable as a solid or in solution at room temperature under an inert atmosphere and does not disproportionate to Cu(II) and copper metal, it is very sensitive to dioxygen.[18]

The X-ray structural analysis of **1** shows that there are two crystallographically independent molecules per asymmetric unit. Each molecule consists of one discrete complex monocation and one PF_6^- anion. A summary of crystal and refinement data is given in Table I with final positional parameters in Table II; selected bond distances and angles are found in Table III. The structure of the $[Cu_2(XYL\text{-}O\text{-})]^+$ cation is shown in Figure 2. Each Cu(I) atom in the dinuclear unit is ligated to the amine nitrogen and two pyridine donors of the py2 tridentate group while the fourth donor is the bridging phenoxo oxygen atom. The geometry about each Cu(I) ion is best described as trigonal pyramidal, similar to that found in Cu(I) complexes of pyridyl-containing tripodal tetradentate ligands.[19] The basal plane is defined by the two pyridine nitrogen atoms and the oxygen atom, with the tertiary amino nitrogen atom in the apical position. Cu(3) lies 0.32 Å above its basal plane formed by N(8), N(9), and O(2),

Table I. Crystallographic Data for Complexes **1** and **3b**

	1	**3b**
temp, K	294	294
a, Å	13.861 (4)	13.410 (3)
b, Å	13.482 (8)	14.867 (3)
c, Å	16.956 (5)	18.990 (4)
α, deg	90.0	102.35 (2)
β, deg	98.20 (2)	91.71 (2)
γ, deg	90.0	98.68 (2)
V, Å^3	7323.61	3648.4
$F(000)$	3447.2	1552
Z	8 (2 per asymmetric unit)	2
D_{calcd}, g/cm^3	1.53	1.32
D_{expti},[a] g/cm^3	1.46	
crystal dimens, mm	0.30 × 0.20 × 0.60	0.20 × 0.20 × 0.50
space group	$P2_1/n$	$P\bar{1}$
scan rate, deg/min	5.0–30.0	15.0–30.0
scan range, deg	0.0–40.0	0.0–40.0
bkgd measurement	stationary crystal, stationary counter, at the beginning and end of each 2θ scan, each for the time taken for the scan	
reflctns measd	$+h,+k,\pm l$	$+h,\pm k,\pm l$
reflctns collected	6979	7417
independent reflctns	2927, with $I_o \geq 3\sigma(I_o)$	2324, with $I_o \geq 3\ 3\sigma(I_o)$
abs coeff, cm^{-1}	12.74	8.56
abs correctn	not applied	not applied
atom scattering factors[b]	neutral atomic scattering factors were used throughout the analysis	
anomalous dispersn[c]	applied to all non-hydrogen atoms	
R[d]	0.0588	0.0990
R_w[d]	0.0587	0.0968
goodness of fit[e]	1.469	2.164

[a] Flotation. [b] Cromer, D. T.; Mann, J. B. *Acta Crystallogr., Sect A: Cryst. Phys., Diffr., Theor. Gen. Crystallogr.* **1968**, *A24*, 321. [c] *International Tables for X-ray Crystallography*: Kynoch Press: Birmingham, England. [d] $R = \sum[(|F_o| - |F_c|/\sum|F_o|]$; $R_w = [\sum w(|F_o| - |F_c|)/\sum w|F_o|^2]^{1/2}$; $w = 1/\delta^2(F_o) + g^*(F_o)^2$; $g = 0.001$. [e] GOF = $[\sum w(|F_o| - |F_c|)^2/(NO - NV)]^{1/2}$, where NO is the number of observations and NV is the number of variables.

toward N(7), while Cu(4) lies 0.29 Å out of its basal plane comprised of N(11), N(12), and O(2) in the direction of N(10). By contrast, Cu(3) sits 0.75 Å above the N(7), N(8), N(9) best least-squares plane and Cu(4) is 0.59 Å below the N(10), N(11), N(12) plane. The dihedral angles about the copper atoms are close to 90° indicative of the trigonal-pyramidal nature of the coordination: N(7), Cu(3), O(2)/N(8), N(9), Cu(3) = 88.1°; N(7), Cu(3), N(8)/N(9), Cu(3), O(2) = 83.9°; N(11), Cu(4), N(12)/O(2), Cu(4), N(10) = 87.6°; N(11), Cu(4), N(10)/N(12), Cu(4), O(2) = 93.4°; O(2), Cu(4), N(11)/N(10), Cu(4), N(12) = 95.3°. The chelating nature of the ligands cause some distortion from idealized pyramidal geometry; the N_{amino}–Cu–N_{py} angles (Table III) are smaller (96–104°) than the N_{py}–Cu–N_{py} angles (107–143°).

The py2 tridentate group can form a wide variety of structural types with Cu(I) or Cu(II). In **1**, the two pyridine donors occupy basal sites in a trigonal pyramid with the N_{py}–Cu–N_{py} angle varying widely between 107 and 143°. Corresponding angles of between 112 and 121° are found in Cu(tepa)$^+$ (tepa = tris(2-(2-pyridyl)ethyl)amine),[19] while angles of 150–158° are found in three-coordinate Cu(I) structures.[17,20] In Cu(II) complexes, the two pyridine donors can be essentially trans in square-planar,[21] square-based pyramidal,[17,19a] or trigonal-bipyramidal[22] structures

(17) Karlin, K. C.; Hayes, J. C.; Gulineh, Y.; Cruse, R. W.; McKown, J. W.; Hutchinson, J. P.; Zubieta, J. *J. Am. Chem. Soc.* **1984**, *106*, 2121–2128.
(18) Anaerobic solutions of **1** slowly decompose (days) in CH_2Cl_2 solution, a process which does not interfere with the chemistry described when freshly prepared solutions are used.
(19) (a) Zubieta, J.; Karlin, K. D.; Hayes, J. C. In ref 13, pp 97–108. (b) Karlin, K. D.; Hayes, J. C.; Hutchinson, J. P.; Hyde, J. R.; Zubieta, J. *Inorg. Chim. Acta* **1982**, *64*, L219–L220.
(20) Blackburn, N. J.; Karlin, K. D.; Concannon, M.; Hayes, M. C.; Gulineh, Y.; Zubieta, J. *J. Chem. Soc., Chem. Commun.* **1984**, 939–940.
(21) Karlin, K. D.; Gulineh, Y.; Hayes, J. C.; Zubieta, J. *Inorg. Chem.* **1984**, *23*, 519–521.
(22) (a) Karlin, K. D.; McKown, J. W.; Hayes, J. C.; Hutchinson, J. P.; Zubieta, J. *Trans. Met. Chem.* **1984**, *9*, 405–406. (b) Karlin, K. D.; Dahlstrom, P. L.; DiPierro, L. T.; Simon, R. A.; Zubieta, J. *J. Coord. Chem.* **1981**, *11*, 61.

Table II. Atom Coordinates ($\times 10^4$) and Temperature Factors ($Å^2 \times 10^3$) for Complex **1**

atom	x	y	z	$U_{equiv/iso}$	atom	x	y	z	$U_{equiv/iso}$
Cu(1)	2373 (1)	3320 (1)	9581 (1)	57 (1)	N(11)	2436 (8)	1453 (3)	1282 (6)	49 (5)[a]
Cu(2)	3058 (1)	2323 (1)	8628 (1)	61 (1)[a]	N(12)	4064 (8)	715 (3)	614 (7)	59 (5)[a]
O(1)	2599 (6)	2966 (3)	8664 (5)	56 (4)[a]	C(9)	2641 (11)	-302 (5)	2277 (8)	81 (5)
N(1)	1077 (7)	3643 (3)	8993 (6)	49 (5)[a]	C(10)	2235 (10)	-335 (4)	1427 (8)	57 (4)
N(2)	3297 (7)	3839 (4)	9573 (6)	60 (5)[a]	C(11)	2073 (10)	-693 (5)	979 (9)	69 (5)
N(3)	2071 (7)	3268 (3)	10664 (6)	52 (5)[a]	C(12)	1715 (11)	-701 (5)	218 (9)	75 (5)
N(4)	4079 (8)	2468 (4)	7787 (6)	56 (5)[a]	C(13)	1444 (10)	-319 (4)	-189 (8)	64 (5)
N(5)	2072 (8)	2013 (3)	7927 (6)	55 (5)[a]	C(14)	1587 (10)	69 (4)	225 (8)	50 (4)
N(6)	3959 (8)	2270 (4)	9593 (6)	62 (5)[a]	C(15)	2001 (10)	60 (4)	1025 (8)	50 (4)
C(1)	784 (10)	3386 (4)	8261 (7)	60 (4)	C(16)	1163 (9)	469 (4)	-176 (8)	54 (4)
C(2)	1528 (9)	3364 (4)	7710 (7)	51 (4)	C(81)	-597 (10)	676 (5)	2345 (8)	64 (5)
C(3)	1355 (11)	3537 (4)	6951 (8)	65 (5)	C(82)	-1569 (11)	657 (5)	2417 (8)	79 (5)
C(4)	2040 (11)	3511 (5)	6420 (9)	74 (5)	C(83)	-1896 (11)	242 (4)	2519 (8)	76 (5)
C(5)	2884 (12)	3325 (5)	6676 (8)	76 (5)	C(84)	-1296 (11)	-87 (5)	2549 (8)	77 (5)
C(6)	3146 (10)	3132 (4)	7430 (7)	53 (4)	C(85)	-315 (11)	-18 (5)	2449 (9)	75 (5)
C(7)	2399 (9)	3148 (4)	7943 (7)	43 (4)	C(86)	354 (12)	-384 (6)	2321 (11)	118 (7)
C(8)	4090 (10)	2939 (4)	7697 (8)	59 (5)	C(87)	1210 (11)	-426 (5)	2924 (9)	85 (6)
C(21)	4248 (11)	3763 (5)	9610 (8)	79 (5)	C(91)	1698 (11)	1266 (5)	3272 (10)	84 (5)
C(22)	4939 (12)	4103 (5)	9591 (9)	89 (6)	C(92)	1917 (12)	1544 (6)	3921 (10)	103 (6)
C(23)	4561 (12)	4485 (5)	9507 (9)	81 (5)	C(93)	2522 (12)	1401 (5)	4518 (10)	101 (6)
C(24)	3615 (11)	4585 (5)	9484 (8)	68 (5)	C(94)	2910 (12)	1014 (5)	4540 (10)	96 (6)
C(25)	2984 (9)	4236 (4)	9535 (7)	47 (4)	C(95)	2671 (12)	732 (5)	3836 (10)	96 (6)
C(26)	1943 (9)	4305 (4)	9482 (8)	58 (4)	C(96)	3171 (12)	337 (5)	3721 (10)	103 (6)
C(27)	1275 (10)	4082 (4)	8796 (7)	56 (4)	C(97)	2619 (12)	-62 (5)	3632 (9)	92 (6)
C(31)	2765 (10)	3335 (4)	11285 (7)	56 (4)	C(111)	3010 (11)	1663 (4)	1848 (8)	67 (5)
C(32)	2543 (10)	3430 (4)	12045 (8)	65 (5)	C(112)	2780 (10)	2064 (5)	2128 (8)	69 (5)
C(33)	1614 (10)	3491 (4)	12135 (8)	61 (5)	C(113)	1935 (10)	2244 (5)	1806 (8)	76 (5)
C(34)	897 (10)	3427 (4)	11506 (7)	55 (4)	C(114)	1327 (11)	2034 (5)	1224 (8)	75 (5)
C(35)	1128 (9)	3309 (4)	10778 (7)	45 (4)	C(115)	1606 (11)	1634 (5)	984 (8)	53 (4)
C(36)	376 (10)	3248 (4)	10065 (8)	68 (5)	C(116)	910 (10)	1389 (5)	377 (8)	74 (5)
C(37)	282 (10)	3615 (4)	9503 (8)	68 (5)	C(117)	1351 (10)	1226 (4)	-339 (8)	65 (5)
C(51)	1135 (10)	1998 (5)	8060 (8)	69 (5)	C(121)	4757 (10)	512 (4)	1099 (9)	70 (5)
C(52)	468 (12)	1763 (5)	7594 (9)	84 (5)	C(122)	5644 (12)	390 (5)	858 (9)	91 (6)
C(53)	708 (12)	1544 (5)	6985 (9)	95 (6)	C(123)	5789 (13)	479 (5)	130 (10)	98 (6)
C(54)	1630 (11)	1548 (5)	6810 (9)	84 (5)	C(124)	5106 (12)	665 (5)	-384 (11)	95 (6)
C(55)	2297 (11)	1788 (5)	7304 (9)	69 (5)	C(125)	4213 (11)	784 (5)	-162 (10)	68 (5)
C(56)	3317 (10)	1824 (5)	7097 (9)	74 (5)	C(126)	3434 (10)	993 (5)	-713 (8)	69 (5)
C(57)	3705 (10)	2270 (4)	7016 (7)	64 (5)	C(127)	2476 (9)	740 (4)	-818 (8)	50 (4)
C(61)	3760 (12)	2421 (5)	10304 (8)	74 (5)	P(1)	3451 (4)	2774 (2)	4289 (3)	82 (2)[a]
C(62)	4456 (11)	2476 (5)	10947 (10)	84 (6)	F(11)	3904 (10)	2391 (5)	3934 (7)	201 (8)[a]
C(63)	5414 (11)	2384 (5)	10923 (9)	82 (5)	F(12)	2927 (11)	3120 (4)	4696 (8)	186 (8)[a]
C(64)	5625 (11)	2230 (5)	10197 (8)	74 (5)	F(13)	2598 (10)	2754 (4)	3634 (7)	192 (8)[a]
C(65)	4916 (11)	2169 (5)	9563 (9)	73 (5)	F(14)	2992 (13)	2455 (4)	4761 (10)	236 (10)[a]
C(66)	5121 (12)	1995 (5)	8783 (8)	82 (5)	F(15)	3896 (11)	3117 (7)	3853 (10)	273 (12)[a]
C(67)	5074 (10)	2318 (5)	8114 (8)	69 (5)	F(16)	4347 (10)	2797 (4)	4896 (10)	245 (9)[a]
Cu(3)	1459 (1)	471 (1)	2405 (1)	60 (1)[a]	P(2)	4159 (4)	517 (2)	6807 (3)	88 (2)[a]
Cu(4)	2820 (1)	898 (1)	916 (1)	53 (1)[a]	F(21)	3311 (9)	313 (4)	6249 (7)	175 (7)[a]
O(2)	2090 (7)	435 (3)	1420 (5)	59 (4)[a]	F(22)	4858 (12)	446 (5)	6224 (10)	248 (10)[a]
N(7)	2032 (8)	-135 (4)	2838 (7)	71 (6)[a]	F(23)	3429 (10)	598 (5)	7384 (9)	215 (9)[a]
N(8)	52 (7)	373 (3)	2343 (6)	51 (5)[a]	F(24)	4412 (12)	87 (4)	7176 (10)	230 (9)[a]
N(9)	2048 (8)	879 (4)	3241 (7)	67 (5)[a]	F(25)	3932 (9)	941 (3)	6347 (7)	154 (6)[a]
N(10)	1879 (7)	819 (3)	-202 (6)	46 (5)[a]	F(26)	4922 (10)	757 (5)	7389 (7)	197 (8)[a]

[a] Equivalent isotropic U defined as one-third of the trace of the orthogonalized U_{11} tensor.

with N_{py}–Cu–N_{py} = 168–178°,[17,19a,21] while axial–equatorial angles in the same coordination types vary between 94 and 103°.[17,19a,23]

The bond distances (Table III) are within the range observed for other Cu(I) complexes with nitrogen donors[17,19,20] and are consistent with both the oxidation state, coordination number, and the coordination geometry.[17] The Cu–N_{py} bond length average of 1.97 Å in the tetracoordinate complex **1** is larger than the Cu–N_{py} values (1.87–1.93 Å) found in two other copper(I) three-coordinate structures of the py2 tridentate group (e.g., complex II[17] and a mononuclear analogue[20]). However, in the tetracoordinate Cu(I) complex, Cu(tepa)$^+$, the equatorial Cu–N_{py} distances are 2.01–2.02 Å and these values are also found in a trigonal-pyramidal environment.[19] Copper–N_{py} bond lengths in Cu(II) structures with py2 are generally found to be close to the 2.0–2.1 Å range;[19-23] although shorter distances are to be expected for the Cu(II) compared to Cu(I) complexes, the copper(II) structures are usually pentacoordinate accounting for the longer bond lengths. The Cu–N_{py}, Cu–N_{amine}, and Cu–$O_{phenoxo}$ bond distances in **1** are very similar to those observed in both an analogous dinuclear complex that contains pyrazole donors,[24] as well as its mononuclear analogue.[25]

There is an "open" coordination site in the structure of **1**, a potential binding site on each Cu(I) ion that is trans to the amino nitrogen atoms (N(7) or N(10)) and which would be in an axial site of a trigonal-bipyramidal structure. For an additional single atom donor to bridge the two copper ions (as in doubly bridged dicopper(II) structures such as III and possibly in **2**) would require that the vacant position trans to the amino nitrogen atoms N(7) and N(10) be one and the same as is the case in the hydroxo-bridged complex III. However, such a coordination site for Cu3 is not identical with that for Cu(4) due to the twisting of the py2 units relative to one another such that in **1**, one py2 tridentate is essentially entirely above the plane of the xylyl connecting unit

(23) Karlin, K. D.; Farooq, A.; Hayes, J. C.; Cohen, B. I.; Zubieta, J., submitted for publication in *Inorg. Chem.*

(24) Sorrell, T. N.; Borovik, A. S. *J. Chem. Soc., Chem. Commun.* **1984**, 1489–1490.

(25) Sorrell, T. N.; Borovik, A. S.; Shen, C.-C. *Inorg. Chem.* **1986**, *25*, 590–591.

Table III. Selected Bond Distances (Å) and Angles (deg) for 1

Interatomic Distances			
Cu(1)–N(1)	2.178 (10)	Cu(1)–N(2)	2.077 (11)
Cu(1)–N(3)	1.948 (10)	Cu(1)–O(1)	1.974 (9)
Cu(2)–N(4)	2.195 (11)	Cu(2)–N(5)	1.943 (10)
Cu(2)–N(6)	1.918 (10)	Cu(2)–O(1)	2.125 (9)
Cu(1)–Cu(2)	3.715		
Cu(3)–N(7)	2.156 (12)	Cu(3)–N(8)	1.962 (11)
Cu(3)–N(9)	1.999 (11)	Cu(3)–O(2)	1.995 (9)
Cu(4)–N(10)	2.158 (10)	Cu(4)–N(11)	1.953 (11)
Cu(4)–N(12)	1.955 (12)	Cu(4)–O(2)	2.03 (19)
Cu(3)–Cu(4)	3.619		
Interatomic Angles			
N(1)–Cu(1)–N(2)	95.7 (2)	N(1)–Cu(1)–N(3)	101.4 (4)
N(2)–Cu(1)–N(3)	106.7 (4)	O(1)–Cu(1)–N(1)	96.7 (4)
O(1)–Cu(1)–N(2)	105.8 (4)	O(1)–Cu(1)–N(3)	140.8 (4)
Cu(1)–O(1)–Cu(2)	130.0 (4)	O(1)–Cu(2)–N(4)	92.6
O(1)–Cu(2)–N(5)	108.0 (4)	O(1)–Cu(2)–N(6)	102.7 (4)
N(4)–Cu(2)–N(5)	99.7 (4)	N(4)–Cu(2)–N(6)	99.8 (4)
N(5)–Cu(2)–N(6)	142.5 (5)		
N(7)–Cu(3)–N(8)	101.2 (4)	N(7)–Cu(3)–N(9)	103.5 (4)
N(8)–Cu(3)–N(9)	116.2 (5)	O(2)–Cu(3)–N(7)	92.9 (4)
O(2)–Cu(3)–N(8)	119.8 (4)	O(2)–Cu(3)–N(9)	116.5 (4)
Cu(3)–O(2)–Cu(4)	128.0 (4)	N(10)–Cu(4)–N(11)	103.0 (4)
N(10)–Cu(4)–N(12)	100.4 (4)	N(11)–Cu(4)–N(12)	129.7 (5)
O(2)–Cu(4)–N(10)	90.7 (4)	O(2)–Cu(4)–N(11)	109.5 (4)
O(2)–Cu(4)–N(12)	114.2 (4)		

while the other is found below this plane. This description can be quantified somewhat by examining the dihedral angle formed between the Cu(3), Cu(4), O(2) plane and the benzene ring carbons C(10)–C(15) (C(3),O(2),Cu(4)/C(10)–C(15) = 53.1°) and the pseudotorsion angle N(7),Cu(3),C(4),N10) which is 106.1°. By contrast, in complex III the distortion is far less and the environment here can be described as two coplanar square-planar CuL_4 units (with a fifth pyridine ligand bound weakly in an axial position) which share an edge and with the exogenous OH^- ligand trans to the two amino nitrogen atoms (idealized N_{amino},Cu(1),Cu(2),N_{amino} pseudotorsion angle is 0°); the dihedral angle Cu(1),$O_{phenoxo}$,Cu(2)/benzene ring = 28.9° and the corresponding N_{amino},Cu(1),Cu(2),N_{amino} pseudotorsion angle is 37.6°. Thus, a potential monoatomic bridging ligand donor (e.g., X^-) could not bind in the "open" site to complex **1** with the geometry observed here. However, examination of models of **1** show that a peroxo (O_2^{2-}) donor as a μ-1,2 ligand could fit very nicely into the existing structure, **1**.

Oxygenation of $[Cu_2(XYL\text{-}O\text{–})]^+$ (1) To Give $[Cu_2(XYL\text{-}O\text{–})(O_2)]^+$ (2). The striking structural features of complex **1** which suggested that it might be suitable for dioxygen binding and as a biomimic of hemocyanin were (a) the observed Cu···Cu distance of 3.6–3.7 Å which is known from EXAFS studies to be the distance in oxy-Hc and (b) the occurrence of an empty "pocket" (Figure 2) in the area where a second bridging ligand (X^-) such as OH^-,[17,23] N_3^-,[23,26,27] Cl^-,[23,26] Br^-,[23,26] and RCO_2^-[23] is known to coordinate in phenoxo-bridged dicopper(II) complexes of XYL-O–. The dinuclear Cu(I) center in **1** would be suitable for binding of O_2 by means of a two-electron redox process and coordination of the resulting peroxo moiety.

When the orange (λ_{max} = 320 (ϵ 9100), 385 nm (ϵ 10 500 $(M\cdot cm)^{-1}$) (Figure 3) dichloromethane solution of **1** is exposed to O_2 below −50 °C, an intense purple color develops due to the formation of the peroxo–Cu^{II}_2 complex **2** (Figure 1).[16]

$$[Cu_2(XYL\text{-}O\text{–})]^+ + O_2 \xrightarrow{CH_2Cl_2,\ -80\ °C} [Cu_2(XYL\text{-}O\text{–})(O_2)]^+$$

Manometric measurements at −80 °C indicate that 1 mol of dioxygen is taken up per mol of **1** to give the product formulated as **2**. The visible spectrum (Figure 3) of the purple solution exhibits a new strong absorption at 505 nm (ϵ 6000 $(M\cdot cm)^{-1}$)

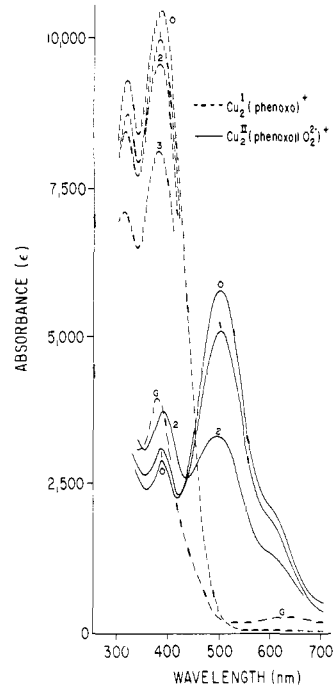

Figure 3. Visible absorption spectrum of the dioxygen (peroxo) complex **2** (solid curve 0) and vacuum cycling experiments demonstrating the quasi-reversible binding nature of dioxygen in this system. The dicopper(I) precursor complex **1** is dissolved in CH_2Cl_2 and the spectrum (dotted spectrum 0) recorded at −80 °C. Exposure to dioxygen ($Cu:O_2$ = 2:1) gives **2** (solid curve 0). Application of a vacuum to this solution while warming removes O_2 and affords the starting compound **1** (dotted curve 1). Oxygenation gives **2** with some decomposition evident (solid curve 1), and removal of dioxygen in vacuo again gives **1** (dotted curve 2). One more repetition of this process gives **2** (solid curve 2) and **1** (dotted curve **3**). Allowing the dioxygen complex **2** to decompose by warming to room temperature, recooling to −80 °C, and recording the spectrum gives the curve labeled G, which matches the known spectrum of the phenoxo and hydroxo doubly bridged dicopper(II) complex III. See text for further explanation and discussion.

and a shoulder at ca. 610 nm (ϵ 2100 $(M\cdot cm)^{-1}$). In addition, there is a band at 385 nm (ϵ 2900 $(M\cdot cm)^{-1}$ (Figure 3) and weaker absorptions in the near-infrared region at 790 (ϵ 700) and 925 nm (ϵ 600 $(M\cdot cm)^{-1}$). The spectral features associated with the formation of the purple-colored **2** are only observed at low temperature (below ca. −50 °C) and only in the presence of O_2. An analysis of the resonance Raman spectroscopic properties of the dioxygen adduct **2** shows that the stronger absorptions at 505 and 610 nm can be assigned as σ and π charge-transfer transitions, respectively, of the coordinated peroxo unit.[28] The absorption at 385 nm is most likely due to the presence of a coordinated phenoxo unit in **2** since this is the prominent charge-transfer band observed in the related phenoxo– and hydroxo–dicopper(II) complex III while the near-infrared features in **2** are probably d–d absorptions that are found at low energy due to coordination distortions and the presumably weak ligand field effect of a peroxo ligand.

Reversible Binding of O_2. Vacuum Cycling. The reversibility of dioxygen binding to **1** is indicated by several lines of evidence including the ability to oxygenate **1** and deoxygenate **2** through several cycles in a quasi-reversible manner without severe decomposition. This is accomplished by the application of a vacuum to a CH_2Cl_2 solution of **2** to remove the bound dioxygen (peroxo) ligand, and this process can be followed spectrophotometrically as shown in Figure 3. Beginning with the pure dicopper(I) complex **1** (spectrum 0, dotted curve), oxygenation at −80 °C gives the spectrum of complex **2** (spectrum 0, solid curve). Rapid warming to room temperature under vacuum removes O_2, regenerating the deoxy complex **1** (spectrum 1, dotted). Lowering

(26) Karlin, K. D.; Hayes, J. C.; Hutchinson, J. P.; Zubieta, J. *J. Chem. Soc., Chem. Commun.* **1983**, 376–378.
(27) Karlin, K. D.; Cohen, B. I.; Hayes, J. C.; Farooq, A.; Zubieta, J. *Inorg. Chem.* **1987**, *26*, 147–153.
(28) Pate, J. E.; Cruse, R. W.; Karlin, K. D.; Solomon, E. I. *J. Am. Chem. Soc.*, in press.

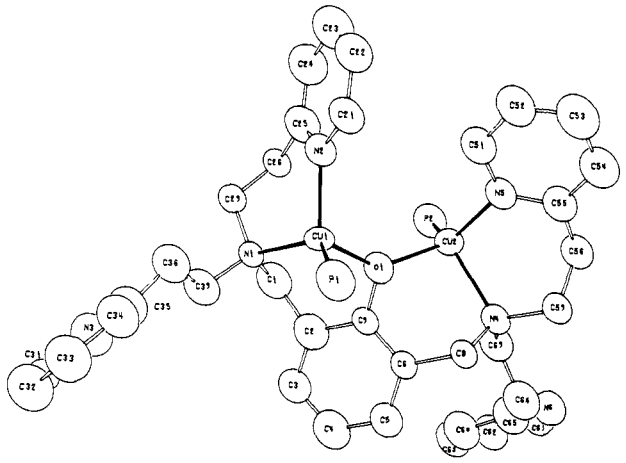

Figure 4. ORTEP diagram of the cationic portion of the bis(triphenylphosphine) adduct **3b** showing the atom labeling scheme in this phenoxo-bridged dicopper(I) complex. The phenyl groups of the PPh_3 ligands are omitted for clarity, and a full ORTEP diagram is available as supplementary material.

the temperature again to −80 °C and bubbling the solution with O_2 regenerate the oxy compound **2** (solid curve 1) with a small amount of decomposition (about 10% as judged by the decrease in absorbance at 500 nm, Figure 3). The cycle can be repeated, as shown, although with a greater degree of decomposition.

We have also confirmed that there is a gas removed when a vacuum is applied to solutions of **2** as described and that it is dioxygen. The *vacuum cycling* experiments can also be carried out and visualized on the benchtop under synthetic conditions (solutions ca. 10^{-3} M).[29] The CH_2Cl_2 solution of **2** is rapidly heated under a static vacuum, and the dioxygen liberated is trapped in an empty flask attached, which is immersed in liquid nitrogen. If the orange solution of **1** so produced is now chilled to −80 °C and the trapped gas on the other side is allowed to warm up, the purple color is restored, indicating formation of **2**. This process can be repeated several cycles before the distinctly green decomposition product is observable. The gas liberated from heating the solution of **2** under vacuum is identified as O_2 by its reaction with a colorless solution of aqueous alkaline pyrogallol (1,2,3-trihydroxybenzene), which is an analytical reagent used to test for dioxygen and which turns to a dark brown color upon exposure to O_2.[29-31]

The UV–VIS spectrum of the solution of **2** that has been allowed to warm up to room temperature has an absorption maximum at 380 nm (Figure 3, spectrum G (dot–dash)). This is the same as a spectrum of the hydroxo and phenoxo doubly bridged dicopper(II) complex $[Cu_2(XYL\text{-}O\text{-})(OH)]^{2+}$ (III),[17] with a solution of an equivalent concentration. As more decomposition occurs upon repeated *vacuum cycling*, the absorption in the 380-nm region of the oxygenated complex increases (Figure 3), approaching that observed for complex III (spectrum G). There also appears to be an isosbestic point present at ca. 450 nm, and the combined results and stoichiometry of reaction suggest that the primary decomposition pathway of the dioxygen complex **2** is that of a disproportionation,[5,32,33] giving III. We have not attempted to isolate III via this route; since **2** is a monocation and III is a dication with a hydroxo bridging group, the decomposition reaction probably also involves attack of the solvent dichloromethane.[33,34] The fate of the dioxygen ligand, the source of the hydroxo oxygen atom in III, and the identity of the second anion in solutions (e.g., OH^-, Cl^-?) derived from the decomposition of **2** have not been determined.

$$[Cu_2(XYL\text{-}O\text{-})]^+ \overset{O_2}{\rightleftharpoons} [Cu_2(XYL\text{-}O\text{-})(O_2)]^+ \rightarrow [Cu_2(XYL\text{-}O\text{-})(OH)]^{2+}$$

Carbon Monoxide and Triphenylphosphine Adducts. The potential ligands (L) carbon monoxide and/or triphenylphosphine both react with **2** resulting in the liberation of O_2 and the formation of **3**. These observations represent further evidence for the reversible nature of dioxygen binding by **1** (Figure 1). The carbonyl adduct **3a** and the triphenylphosphine adduct **3b** have also been prepared by the direct reaction of **1** with L. Thus, bubbling CO through a dichloromethane solution of **1** results in a color change from orange to a pale yellow. The IR spectrum of the carbonyl

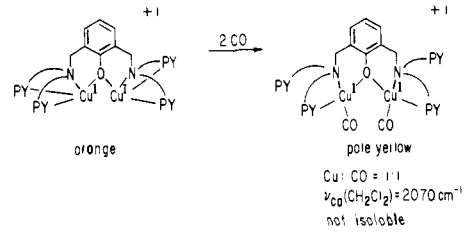

adduct so formed in solution exhibits $\nu(CO) = 2070\ cm^{-1}$ which is in the range expected for coordinated CO.[33-35] However, compound **3a** cannot be isolated as a solid even under 1 atm of CO; attempts to do this result only in the recovery of **1**. The stoichiometry of adduct formation is confirmed by manometric measurements at −80 °C which indicate that 2 mol of CO are taken up per mol of dicopper(I) complex **1** in dichloromethane.

The X-ray structure analysis of the phosphine adduct **3b** is shown in Figure 4, and it shows that this complex consists of a dinuclear center with tetracoordinate Cu(I) and uncoordinated "dangling" pyridine-containing arms from the ligand. Although NMR data are unavailable at this time, the solution structures for both **3** and **3b** are likely to be the same, since the solution infrared spectrum observed for **3a** confirms CO coordination; for all of the pyridine donors to coordinate would require pentacoordination for copper which is relatively rare in Cu(I) complexes.[36]

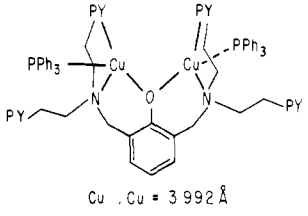

Structure of $[Cu_2(XYL\text{-}O\text{-})(PPh_3)_2](PF_6)$ (3b). Compound **3b** was crystallized as a CH_2Cl_2 solvate, and the X-ray crystal structure (Table I) of the cation is shown in Figure 4. The phenyl

(29) Cruse, R. W. Ph.D. Thesis, State University of New York at Albany, 1986.

(30) Gordon, A. J.; Ford, R. A. *The Chemist's Companion, A Handbook of Practical Data, Techniques and References*; Wiley: New York, 1972; p 440.

(31) The quantity of gas released on the first cycle was determined by transferring the O_2 trapped at liquid-nitrogen temperature in a small (5-mL) bulb attached via capillary tubing to a stopcock and then measuring the volume of gas (at 0 °C) on the constant-pressure manometric apparatus.[29] After the vapor pressure due to the solvent was corrected for, 70–80% of the O_2 expected to be bound to copper in complex **2** was recovered by using this method.

(32) Thompson, J. S. *J. Am. Chem. Soc.* **1984**, *106*, 8308–8309.

(33) Thompson, J. S. In ref 14, pp 1–10.

(34) Thompson, J. S. *J. Am. Chem. Soc.* **1984**, *106*, 4057–4059.

(35) (a) Nelson, S. M.; Lavery, A.; Drew, M. G. B. *J. Chem. Soc., Dalton Trans.* **1986**, 911–920. (b) Thompson, J. S.; Swiatek, R. M. *Inorg. Chem.* **1985**, *24*, 110–113. (c) Thompson, J. S.; Whitney, J. F. *Inorg. Chem.* **1984**, *23*, 2813–2819. (d) Sorrell, T. N.; Malachowski, M. R. *Inorg. Chem.* **1983**, *22*, 1883–1887. (e) Gagne, R. R.; Kreh, R. P.; Dodge, J. A.; Marsh, R. E.; McCool, M. *Inorg. Chem.* **1982**, *21*, 254–261. (f) Kitagawa, S.; Munakata, M. *Inorg. Chem.* **1981**, *20*, 2261–2267. (g) Casella, L.; Ghelli, S. *Inorg. Chem.* **1983**, *22*, 2458–2463. (h) Pasquali, M.; Floriani, C.; Venturi, G.; Gaetani-Manfredotti, A.; Chiesi-Villa, A. *J. Am. Chem. Soc.* **1982**, *104*, 4092 and references therein.

(36) Gagne, R. R.; Koval, C. A.; Smith, T. J.; Cimolino, M. C. *J. Am. Chem. Soc.* **1979**, *101*, 4571. (b) Gagne, R. R.; Allison, J. L.; Ingle, D. M. *Inorg. Chem.* **1979**, *18*, 2767. (c) Drew, M. G. B.; Cairns, C.; McFall, S. G.; Nelson, S. M. *J. Chem. Soc., Dalton Trans.* **1980**, 2020.

Table IV. Atom Coordinates ($\times 10^4$) and Temperature Factors ($Å^2 \times 10^3$) for Complex **3b**

atom	x	y	z	$U_{equiv/iso}$	atom	x	y	z	$U_{equiv/iso}$
Cu(1)	8083 (3)	2963 (2)	1449 (2)	40 (1)[a]	C(103)	8536 (14)	2216 (8)	-1201 (8)	75 (9)
Cu(2)	6334 (3)	2224 (2)	2962 (2)	44 (1)[a]	C(104)	8467 (14)	1315 (8)	-1625 (8)	70 (9)
P(1)	8859 (7)	1861 (4)	853 (3)	44 (3)[a]	C(105)	8504 (14)	565 (8)	-1297 (8)	54 (8)
P(2)	5727 (7)	3322 (5)	3712 (3)	50 (4)[a]	C(106)	8611 (14)	716 (8)	-546 (8)	53 (8)
O(1)	7622 (13)	2711 (9)	2470 (7)	39 (7)[a]	C(101)	8680 (14)	1616 (8)	-123 (8)	29 (7)
N(1)	8702 (17)	4374 (11)	1963 (8)	34 (6)	C(112)	9078 (11)	196 (12)	1256 (7)	63 (9)
N(4)	7108 (18)	1202 (11)	3359 (9)	47 (6)	C(113)	8716 (11)	-678 (12)	1388 (7)	64 (9)
C(1)	8643 (24)	4532 (16)	2753 (11)	71 (9)	C(114)	7681 (11)	-1013 (12)	1316 (7)	58 (9)
C(2)	9096 (15)	3712 (10)	3005 (8)	70 (9)	C(115)	7006 (11)	-473 (12)	1111 (7)	61 (9)
C(3)	10013 (15)	3867 (10)	3413 (8)	61 (9)	C(116)	7367 (11)	402 (12)	978 (7)	44 (8)
C(4)	10308 (15)	3157 (10)	3706 (8)	78 (10)	C(111)	8403 (11)	736 (12)	1051 (7)	41 (8)
C(5)	9685 (15)	2291 (10)	3592 (8)	59 (9)	C(122)	10607 (14)	2319 (9)	1725 (8)	47 (8)
C(6)	8767 (15)	2136 (10)	3185 (8)	40 (7)	C(123)	11639 (14)	2393 (9)	1896 (8)	85 (11)
C(7)	8473 (15)	2847 (10)	2891 (8)	39 (7)	C(124)	12290 (14)	2167 (9)	1349 (8)	67 (9)
C(8)	8108 (21)	1207 (14)	3047 (11)	50 (8)	C(125)	11909 (14)	1867 (9)	632 (8)	61 (9)
C(21)	6379 (14)	2533 (9)	339 (8)	59 (8)	C(126)	10876 (14)	1793 (9)	461 (8)	60 (9)
C(22)	5471 (14)	2634 (9)	10 (8)	69 (9)	C(121)	10225 (14)	2019 (9)	1007 (8)	31 (7)
C(23)	5017 (14)	3413 (9)	275 (8)	89 (10)	C(202)	6394 (12)	5265 (12)	3975 (7)	51 (8)
C(24)	5471 (14)	4090 (9)	869 (8)	84 (10)	C(203)	7132 (12)	6052 (12)	4208 (7)	83 (10)
C(25)	6379 (14)	3989 (9)	1198 (8)	67 (9)	C(204)	8060 (12)	5968 (12)	4517 (7)	70 (9)
N(2)	6833 (14)	3211 (9)	933 (8)	50 (6)	C(205)	8251 (12)	5096 (12)	4594 (7)	72 (10)
C(26)	6943 (21)	4674 (15)	1825 (11)	44 (8)	C(206)	7514 (12)	4309 (12)	4361 (7)	66 (9)
C(27)	8004 (22)	4977 (16)	1739 (13)	59 (9)	C(201)	6586 (12)	4393 (12)	4051 (7)	41 (7)
C(31)	12599 (17)	5610 (10)	1096 (9)	95 (12)	C(212)	4580 (14)	3809 (11)	2634 (9)	81 (10)
C(32)	12973 (17)	5042 (10)	515 (9)	88 (11)	C(213)	3811 (14)	4206 (11)	2367 (9)	75 (10)
C(33)	12336 (17)	4279 (10)	88 (9)	85 (11)	C(214)	3092 (14)	4545 (11)	2825 (9)	83 (10)
C(34)	11326 (17)	4085 (10)	242 (9)	74 (10)	C(215)	3142 (14)	4487 (11)	3548 (9)	78 (10)
C(35)	10952 (17)	4653 (10)	823 (9)	69 (10)	C(216)	3911 (14)	4090 (11)	3814 (9)	58 (9)
N(3)	11588 (17)	5416 (10)	1251 (9)	83 (8)	C(211)	4629 (14)	3751 (11)	3357 (9)	42 (7)
C(36)	9888 (23)	4534 (17)	968 (12)	69 (9)	C(222)	4470 (15)	2155 (12)	4359 (7)	90 (11)
C(37)	9741 (24)	4678 (17)	1767 (12)	62 (9)	C(223)	4116 (15)	1761 (12)	4927 (7)	88 (11)
C(51)	5128 (14)	1427 (9)	1579 (8)	66 (9)	C(224)	4532 (15)	2139 (12)	5629 (7)	87 (11)
C(52)	4477 (14)	756 (9)	1077 (8)	76 (10)	C(225)	5300 (15)	2911 (12)	5764 (7)	70 (9)
C(53)	4114 (14)	-104 (9)	1233 (8)	91 (11)	C(226)	5654 (15)	3305 (12)	5196 (7)	66 (9)
C(54)	4401 (14)	-295 (9)	1891 (8)	83 (10)	C(221)	5238 (15)	2927 (12)	4494 (7)	46 (8)
C(55)	5053 (14)	376 (9)	2393 (8)	65 (9)	P(3)	5519 (11)	7133 (5)	2066 (5)	99 (6)[a]
N(5)	5416 (14)	1237 (9)	2237 (8)	53 (6)	F(1)	4964 (18)	6272 (13)	1483 (10)	141 (8)
C(56)	5370 (22)	251 (16)	3090 (11)	61 (9)	F(2)	5664 (18)	6502 (12)	2592 (9)	127 (7)
C(57)	6494 (20)	219 (14)	3179 (12)	49 (8)	F(3)	5440 (17)	7800 (12)	1551 (9)	123 (7)
C(61)	7195 (17)	1933 (18)	6572 (12)	120 (13)	F(4)	6105 (19)	7974 (14)	2624 (10)	138 (8)
C(62)	7885 (17)	2759 (18)	6770 (12)	121 (13)	F(5)	6574 (21)	6913 (15)	1715 (11)	172 (9)
C(63)	8555 (17)	3024 (18)	6275 (12)	184 (19)	F(6)	4560 (26)	7398 (19)	2444 (14)	220 (13)
C(64)	8536 (17)	2463 (18)	5584 (12)	117 (13)	C(11)	908 (56)	57 (38)	3529 (27)	60 (21)
C(65)	7846 (17)	1636 (18)	5386 (12)	84 (10)	Cl(1)	1129 (36)	640 (26)	4306 (19)	260 (19)
N(6)	7176 (17)	1371 (18)	5880 (12)	155 (13)	Cl(2)	2174 (28)	814 (19)	3186 (15)	175 (12)
C(66)	7764 (26)	1077 (17)	4629 (12)	82 (10)	C(12)	8641 (64)	8042 (51)	3199 (32)	246 (41)
C(67)	7185 (24)	1586 (16)	4164 (11)	69 (9)	Cl(3)	9319 (19)	7667 (13)	2632 (10)	175 (8)
C(102)	8643 (14)	2367 (8)	-450 (8)	48 (8)	Cl(4)	8611 (22)	8560 (15)	3899 (11)	218 (10)

[a] Equivalent isotropic U defined as one-third of the trace of the orthogonalized U_{ij} tensor.

groups of the PPh_3 ligands are omitted for clarity, but a full ORTEP drawing of the entire cation is available in the supplementary material. Final positional parameters are given in Table IV, and selected bond distances and angles are found in Table V. Each Cu(I) ion in the structure is tetracoordinate with a pseudotetrahedral geometry. Ligation occurs to the amino nitrogen and one pyridine arm of the py2 tridentate unit, the phenoxo oxygen atom and the phosphorous atom of the triphenylphosphine ligand. The presence of one "dangling" uncoordinated pyridine group from each py2 unit is seen clearly in Figure 4. The two halves of the molecule can be seen as related by a noncrystallographic twofold axis running through O(1), C(7) and C(4), but distinct differences in corresponding bond lengths and angles (Table IV) and dihedral angles exist (e.g., N(1),Cu(1),N(2)/O(1),Cu(1),P(1) = 79° while N(4),Cu(2),N(5)/O(1),Cu(2),P(2) = 100°). As in compound **1**, twisting of the py2 units result in the Cu···Cu vector lying across the benzene ring with the dihedral angle Cu(1),O(1),Cu(2)/C2–C7 = 57.8°. The pseudotorsion angle N(1)–Cu(1)–Cu(2)–N(4) is 110.5°. The Cu···Cu distance is quite long in **3b** (3.992 Å) which probably is due to the steric crowding of the PPh_3 ligands at the dinuclear coordination center. Accordingly, the Cu(1)–O(1)–Cu2 angle is also large (140.8 (8)°) compared to the corresponding angle (129° average) in **1**. The Cu–O(1) distance is 2.12 Å (average), which is significantly greater than the 2.02-Å average bond length observed in **1**.

Table V. Selected Bond Distances (Å) and Angles (deg) for **3b**

	Interatomic Distances		
Cu(1)–P(1)	2.201 (8)	Cu(2)–P(2)	2.197 (8)
Cu(1)–N(1)	2.143 (15)	Cu(2)–N(4)	2.208 (21)
Cu(1)–N(2)	2.036 (19)	Cu(2)–N(5)	2.014 (14)
Cu(1)–O(1)	2.143 (15)	Cu(2)–O(1)	2.095 (16)
Cu(1)···Cu(2)	3.992		
	Interatomic Angles		
N(1)–Cu(1)–N(2)	98.7 (7)	N(4)–Cu(2)–N(5)	93.6 (6)
N(1)–Cu(1)–O(1)	89.8 (6)	N(4)–Cu(2)–O(1)	92.0 (7)
N(1)–Cu(1)–P(1)	128.8 (7)	N(4)–Cu(2)–P(2)	121.3 (5)
N(2)–Cu(1)–O(1)	106.2 (7)	N(5)–Cu(2)–O(1)	109.8 (6)
N(2)–Cu(1)–P(1)	116.4 (5)	N(5)–Cu(2)–P(2)	121.1 (6)
O(1)–Cu(1)–P(1)	112.6 (5)	O(1)–Cu(2)–P(2)	114.1 (4)
Cu(1)–O(1)–Cu(2)	140.8 (8)		

Reversible Binding of O_2 and CO. Carbonyl Cycling. The binding of CO to **1** is reversible (Figure 1); the CO complex **3a** forms in CH_2Cl_2 (IR evidence, manometry), but the carbon monoxide ligands dissociate and **1** is obtained when attempts are made to isolate **3a**. The carbonylation of **1** is effected by bubbling its CH_2Cl_2 solution with CO while decarbonylation occurs on the application of reduced pressure to dichloromethane solutions of

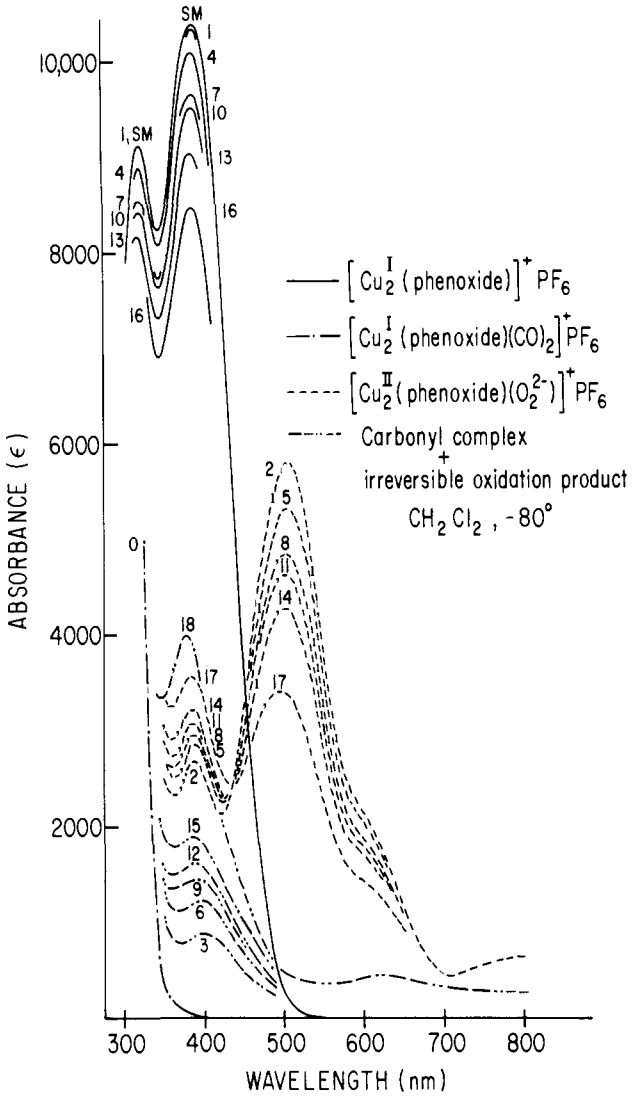

Figure 5. Absorption spectra showing the "carbonyl cycling" behavior where the dioxygen adduct **2** (dotted curve) is reacted with CO to give the dicarbonyl adduct **3a** whereupon CO can be removed in vacuo to give the dicopper(I) complex **1** (solid curves), which can be reoxygenated to give **2**. The experiment starts with complex **1** as the starting material (SM) which is bubbled with CO to produce **3a** (spectrum 0). The CO ligands are removed in vacuo at room temperature giving back **1** (spectrum 1). Oxygenation at −80 °C gives **2** (spectrum 2), and saturation of the solution with CO and slight warming displaces the bound O_2 ligand producing **3a** and some decomposition product (spectrum 3). The process can be repeated, and a total of six cycles are shown. At this point the dioxygen complex **2** was allowed to decompose by warming to room temperature; the resulting product (spectrum 18, −80 °C) is complex III. See text for further explanation and discussion.

3a at room temperature. This process can be followed spectrophotometrically (Figure 5). The spectrum of complex **1** (labeled SM, Figure 5) changes to the featureless spectrum 0, that of the dicarbonyl adduct **3a**, on bubbling the solution with CO. Application of a vacuum to this solution (followed by replenishment with deaerated CH_2Cl_2 solvent to keep the volume constant) restores the spectrum of complex **1** (spectrum 1, Figure 5). This process, **1** + 2CO ⇌ **3a**, can be repeated indefinitely.

In order to produce the dioxygen adduct **2**, it is necessary to start with the dicopper(I) complex **1**, since we observe that at temperatures low enough to stabilize **2** (i.e., −50 °C or less), O_2 will not react with the carbonyl adduct **3a**. The reaction of O_2 with **3a** at room temperature results in the loss of CO with the rapid irreversible oxidation to form III. It is apparent that the binding of CO to **1** is stronger than that of O_2 at −80 °C, and CO can be used to displace the bound dioxygen (peroxo-) ligand, thereby allowing for *carbonyl cycling* to take place (Figure 5).

The solution of complex **1** (spectrum 1, Figure 5), generated as described above, is chilled to −80 °C and bubbled with O_2 to produce **2** (spectrum 2). This solution is saturated with CO by bubbling directly and allowed to warm slightly above −80 °C in the air, with shaking, until the intensely colored purple solution bleaches. Recooling and equilibration at −80 °C gives spectrum 3, which is that characteristic of the bis-carbonyl adduct **3a**, along with some of the decomposition product III. The cycle of decarbonylation of **3a** to give **1**, oxygenation of **1** at low temperature to give **2**, and displacement of O_2 by carbonylation of **2** to give back **3a** (Figure 1) can be repeated many times, as shown in Figure 5. From the absolute decrease in the absorbance of the 505-nm peak of **2** (Figure 5), an estimated 5–15% decomposition occurs per cycle. The decomposition product, with an absorption maximum at 380 nm, builds up with each cycle (spectra 3, 6, 9, 12, 15, Figure 5). After the sixth cycle, the oxygneated solution (spectrum 17) was allowed to warm to room temperature; as in the *vacuum cycling* experiment (Figure 3), the product so formed is identified as the hydroxo and phenoxo doubly bridged complex III (spectrum 18). Also, as in Figure 3, an isosbestic point at ca. 450 nm appears to be evident in the spectrum of the oxygenated species (spectra 2, 5, 8, 11, 14), indicating the presence of a two-species mixture, **2** and III.

Reactions of [Cu$_2$(XYL-O-)(O$_2$)]$^+$ (2) with CO and PPh$_3$. The positive identification of O_2 as the gas liberated from **2** upon the application of a vacuum or on reacting with CO or PPh_3 is an important demonstration of a criterion for reversible binding of dioxygen. Spectrophotometric cycling between oxidized (oxygenated) and reduced forms of a complex could be mistakenly thought to be due to reversible binding of O_2 (to give an O_2 complex). Such behavior might actually arise via the chemical reduction of the oxidized (oxygenated) species (e.g., by a reducing agent such as the solvent or the ligand) to the deoxy (reduced) form of the compound but without the liberation of O_2 (e.g., irreversible reduction and O–O bond cleavage of O_2).[4] In the present system, however, dioxygen is definitely evolved upon reaction of either CO or PPh_3 with **2**.

As described above, bubbling cold solutions of **2** with CO results in the formation of the bis-carbonyl adduct **3a** as followed by UV–vis spectroscopy. Dioxygen is liberated in this process as well, as is shown by using the alkaline pyrogallol test solution (see above). A dichloromethane solution of **2** at −80 °C can be purged of any excess dioxygen in solution by either (a) alternate vacuum-purge cycles under argon or (b) flushing the solution with Ar or CO. When a solution of **2** is now bubbled continuously with carbon monoxide at −80 °C and the gas is passed through a clear and colorless pyrogallol test solution, no change occurs since CO does not displace O_2 from **2** under these conditions. However, when the solution of **2** is warmed up with shaking while bubbling with CO, the test solution rapidly turns brown, indicative of the presence of dioxygen (see Experimental Section).

The O_2 uptake by **1** to form **2** and O_2 released from **2** on adding PPh_3 were also measured by manometry. A CH_2Cl_2 solution of **1** binds 1 mol of O_2/mol of complex to form **2** at −80 °C. When 2 equiv of triphenylphosphine is added to CH_2Cl_2 solutions of **2** at −80 °C, 1 mol of dioxygen/mol of the dicopper dioxygen complex **2** is evolved rapidly and quantitatively. In a separate experiment, an alkaline pyrogallol test solution turns brown when swept with an argon stream which has been passed through a solution of **2** plus triphenylphosphine; this confirms the gas released in the experiment to be O_2. Thus, the reactions of **2** with CO and PPh_3 can be summarized as

$$[Cu_2(XYL\text{-}O\text{-})(O_2)]^+ + 2L\ (L = CO, PPh_3) \rightarrow [Cu_2(XYL\text{-}O\text{-})(L_2)]^+ + O_2$$

Decomposition of the Dioxygen Complex 2. The cycling of O_2 binding to **1** to form **2** and O_2 release by **2** to reform **1** is accompanied by decomposition of **2** to give the hydroxo and phenoxo doubly bridged dicopper(II) complex III which is identified and determined quantitatively by UV–vis spectroscopy. This reaction occurs readily at warmer temperatures, and it is unavoidable under the conditions of the cycling experiments in which either warming

of **2** is required to pump off O_2 or the reaction of **2** with CO effects the displacement of O_2. However, complex III is the only copper decomposition product observed.

The most likely pathway for the decomposition of **2** is via the generation of H_2O_2 or HO_2^- by the reaction of **2** with water or solvent at temperatures above −80 °C, followed by the well-established copper(II)-catalyzed decomposition to water and dioxygen.[32-34,37] This represents an overall reaction of Cu(I) with O_2 in the ratio of Cu(I):O_2 = 4:1.

In a reaction of O_2 with a phenoxo-bridged dicopper(I) complex having pyrazolyl donors and with a design similar to **1**, a 4:1 Cu(I):O_2 reaction stoichiometry is observed even at low temperature, and no evidence for a dioxygen–dicopper complex (peroxo–dicopper(II)) is observed spectroscopically.[24] It is suggested both by Sorrell[24] and by Nelson in an unrelated dicopper system[38] (Cu:O_2 = 4:1, also) that these reactions with a 4Cu(I):O_2 stoichiometry proceed by the fast bimolecular two-electron transfer from a second dicopper(I) molecule to the putative peroxo–dicopper(II) intermediate to give an aggregated oxo–copper(II) product:

$$\mathrm{Cu(I)\cdots Cu(I)} + \mathrm{O_2} \rightleftharpoons \mathrm{Cu(II)\text{-}(O_2^{2-})\text{-}Cu(II)}$$

$$\mathrm{Cu(II)\text{-}(O_2^{2-})\text{-}Cu(II)} + \mathrm{Cu(I)\cdots Cu(I)} \rightarrow 2[\mathrm{Cu(II)\text{-}O\text{-}Cu(II)}]_n$$

This proposal implies that the first step above is kinetically slow compared to the second. As applied to the present system, we can thus speculate that for the reaction of **1** with O_2 at −80 °C in dichloromethane, the reverse situation occurs where the initial reaction of dicopper(I) complex with O_2 is very rapid compared to the ensuing reaction. This being the case, we are able to manipulate and spectroscopically characterize the kinetically stabilized dioxygen adduct (Cu(I):O_2 = 2:1). Apparently, in Sorrell's system, the effect of pyrazolyl ligands (compared to pyridine donors in the present ligand system) is to slow the initial reaction of the dicopper(I) complex with dioxygen. This suggested difference in reactivity rates is supported by the relative redox properties observed for the pyridine-containing *m*-xylyl dicopper(I) complex II and the corresponding identical pyrazolyl analogue of Sorrell's where the $E_{1/2}$ (cyclic voltammetry, CH_3CN) for II is 0.15 V more negative than that of the pyrazolyl complex,[39a] making the pyridine-coordinated Cu(I) species more susceptible to rapid reactions with O_2. These observations are also in accord with the known stronger basicity of pyridine compared to pyrazole derivatives.[39b]

Possible Structures of 2. The coordination environment and mode of binding of the O_2 (peroxo) ligand in **2** is of considerable interest since there is no unambiguously structurally characterized dioxygen adduct of copper known at present.[5] We have so far been unable to isolate a stable solid form of **2**,[40] and this current attempts to define the dioxygen (peroxo) ligand coordination environment require solution studies (e.g., resonance Raman, EXAFS).[28,41] Complex **2** does *not* exhibit an EPR spectrum at 77 K in CH_2Cl_2, consistent with the presence of magnetically coupled bridged (phenoxo and/or peroxo) Cu(II) ions, but additional studies (e.g., magnetic susceptibility) are necessary.

Several possible modes of binding of the peroxo ligand to a dinuclear metal center are known (**a–d**).[4,5,42] The μ-1,2-peroxo coordination to Cu(II) (cis or trans **a**) is suggested for oxy-Hc and has been proposed (by analogy to Hc) in coordination complexes reported by Wilson[44] and Casella.[45] These and other model

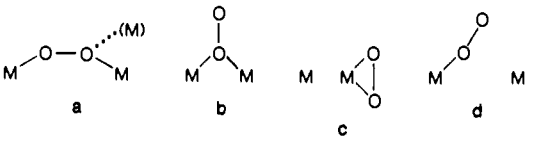

systems[14,32-34,43] are also all reported to bind dioxygen reversibly. The μ-1,2-type of coordination (cis or trans) is also well-established for peroxo- and superoxo–dicobalt(III) compounds.[42] A μ-1,1-peroxo bridging mode (**b**) had been considered and ruled out for oxy-Hc[46] and oxyhemerythrin[47] (non-heme diiron O_2 carrier), but such an entity has been proposed in cobalt systems,[48] and a protonated (hydroperoxo) dicobalt(III) complex with this binding mode has been structurally characterized.[49] The coordination of the peroxo ligand to one copper(II) at the dinuclear center (**c** or **d**) seems unlikely, but such an asymmetrical coordination cannot be ruled out at this time.[28] Terminal peroxo coordination to Fe(III) with protonation and hydrogen bonding to a μ-oxo ligand is the generally accepted coordination mode observed in oxyhemerythrin.[50] Binding modes **a** or **d** are favored as the structure for the dicopper complex **2**, but such conclusions await the results of further studies.[28,41]

Conclusions

We have presented evidence that at low temperature, the reaction of dioxygen with the phenoxo-bridged dicopper(I) complex **1** results in the formation of a bona fide dioxygen/copper adduct [peroxo–dicopper(II), as confirmed by resonance Raman studies[16,28]], **2**, and that the binding is reversible (Figure 1).[43,53] Cycling experiments can be carried out such that O_2 can be removed from **2** by the application of a vacuum, resulting in the regeneration of **1** and the recovery of dioxygen. In addition, CO and PPh_3 react with **2**, liberating O_2 and forming dicopper(I) adducts of CO or PPh_3, **3**. Coordinated CO can be removed from **3a** at room temperature under a partial vacuum, with the regeneration of **1**; subsequent cooling and addition of O_2 results in the reformation of **2**. No oxidation product (e.g., CO_2 or carbonates[53]) of CO has been observed in these reactions. The reaction of **2** with triphenylphosphine at low temperature only results in the displacement of O_2; this behavior contrasts with the observed reaction of a hydroperoxo complex containing XYL-O– (a protonated form of **2**), $[Cu_2(XYL\text{-}O\text{-})(OOH)]^{2+}$, where the quantitative oxidation of triphenylphosphine to $O{=}PPh_3$ occurs.[54a] These results suggest that **2** is *not* a potent oxygenating agent.[54b]

The electronic absorption spectrum of the dioxygen complex **2** is significantly different than that of oxy-Hc; the latter exhibits

(37) Zuberbuhler, A. D. In ref 13, pp 237–258.
(38) Nelson, S. M.; Esho, F. S.; Lavery, A.; Drew, M. G. B. *J. Am. Chem. Soc.* **1983**, *105*, 5693.
(39) (a) Sorrell, T. N.; Malachowski, M. R.; Jameson, D. L. *Inorg. Chem.* **1982**, *21*, 3250–3252. (b) Dedert, P. L.; Thompson, J. S.; Ibers, J. A.; Marks, T. J. *Inorg. Chem.* **1982**, *21*, 969–977 and references therein.
(40) We can isolate a purple powder by precipitating a dichloromethane solution of **2** at −80 °C with diethyl ether. The solid is not thermally stable, however.
(41) Blackburn, N. J.; Strange, R. W.; Cruse, R. W.; Karlin, K. D. *J. Am. Chem. Soc.* **1987**, *109*, 1235–1237.
(42) Gubelmann, M. H.; Williams, A. F. *Struct. Bonding (Berlin)* **1983**, *55*, 1 and references cited therein.
(43) Other copper complex systems that have reported to bind dioxygen reversibly are given in ref 14 and 32–34. In addition, there are: (a) Merrill, C. L.; Wilson, L. J.; Thamann, T. J.; Loehr, T. M.; Ferris, N. S.; Woodruff, W. H. *J. Chem. Soc., Dalton Trans.* **1984**, 2207–2221 and references therein. (b) Casella, L.; Silver, M. S.; Ibers, J. A. *Inorg. Chem.* **1984**, *23*, 1409–1418. (c) Nishida, Y.; Takahashi, K.; Kuramoto, H.; Kida, S. *Inorg. Chim. Acta* **1981**, *54*, L103–L104. (d) Bulkowski, J. E.; Burk, P. L.; Ludmann, M.-F.; Osborn, J. A. *J. Chem. Soc., Chem. Commun.* **1977**, 498–499.
(44) (a) See ref 43a. (b) Goodwin, J. A.; Stanbury, D. M.; Wilson, L. J. In ref 14, pp 11–26.
(45) See ref 43b.
(46) Thamann, T. J.; Loehr, J. S.; Loehr, T. M. *J. Am. Chem. Soc.* **1977**, *99*, 4187.
(47) Kurtz, D. M., Jr.; Shriver, D. F.; Klotz, I. M. *J. Am. Chem. Soc.* **1976**, *98*, 5033.
(48) Durand, R. R., Jr.; Bencosme, C. S.; Collman, J. P.; Anson, F. C. *J. Am. Chem. Soc.* **1983**, *105*, 2710–2718.
(49) Thewalt, U.; Marsh, R. A. *J. Am. Chem. Soc.* **1967**, *89*, 6364–6365.
(50) Stenkamp, R. E.; Sieker, L. C.; Jensen, L. H.; McCallum, J. D.; Sanders-Loehr, J. *Proc. Natl. Acad. Sci. U.S.A.* **1985**, *82*, 713–716.
(51) Karlin, K. D.; Haka, M. S.; Cruse, R. W.; Gultneh, Y. *J. Am. Chem. Soc.* **1985**, *107*, 5828–5829.
(52) Karlin, K. D., and co-workers, manuscript in preparation.
(53) A recent report describes a Cu(II) peroxide complex formed by the reaction of O_2 with $Cu_2L_2I_2$ (L = chelating N-heterocycle) in the presence of 2-methylimidazole: Bhaduri, S.; Sapre, N. Y.; Basu, A. *J. Chem. Soc., Chem. Commun.* **1986**, 197–198.
(54) (a) Karlin, K. D.; Cruse, R. W.; Gultheh, Y. *J. Chem. Soc., Chem. Commun.*, in press. (b) In oxidation reactions with certain substrates, peroxo–dicobalt(III) complexes are inert, whereas the protonated hydroperoxo species is reactive.[42]

features at 345 (ϵ 20 000) and 570 nm (ϵ 1000 M^{-1} cm^{-1}) and a circular dichroic feature at 485 nm, all assignable to LMCT transitions. Thus, while we have been able to establish with certainty that **1** reacts with O_2 to form a dioxygen adduct, **2**, it does not possess features that closely model the spectroscopic properties observed for oxyhemocyanin. We have recently reported that oxygenated dicopper(I) complexes ($Cu:O_2$ = 2:1) of modified ligand systems but possessing py2 tridentate units and connected by groups other than the bridging phenoxo group have UV–vis spectral features that seem to closely resemble those of oxy-Hc.[51,52] These complexes also bind dioxygen reversibly and may presently serve as closer biomimics for Hc.

Collaborative efforts to characterize the spectroscopic and structural properties of **2** are in progress.[28,41] Other current activities include the synthesis of modified forms of the ligand IV, which may enhance the thermal stability of derived analogues of **2**. We are also probing the reactivity of **2** by using substrates which are oxidizable and/or whose reaction products may provide insights into the nature of the bound O_2 ligand.

Experimental Section

Materials and Methods. Reagents and solvents used were of commercially available reagent grade quality. Dioxygen and carbon monoxide gases were dried by passing through a short column of supported P_4O_{10} (Aquasorb, Mallinkrodt) and/or a copper coil tube immersed in a −80 °C cold trap. Methanol was distilled from $Mg(OMe)_2$, and anhydrous diethyl ether was freshly dried by passing it through a 60-cm long column of activated alumina and collected under Ar, or it was directly distilled from sodium/benzophenone. In the dark, CH_2Cl_2 was stirred with concentrated sulfuric acid for several days. After removal of the acid layer, the dichloromethane was washed with a KOH–KCl-(saturated) solution and distilled water and then dried over anhydrous K_2CO_3 or $MgSO_4$ before a final reflux and distillation from CaH_2.

Preparation and handling of air-sensitive compounds were carried out by using standard Schlenk techniques. Deoxygenation of solvents and solutions was carried out by either repeated vacuum/purge cycles (N_2 or Ar) or by bubbling (20 min) with N_2 or Ar. Solid samples were stored and transferred, and samples for infrared (IR) and NMR spectra were prepared in a Vacuum/Atmospheres drybox filled with argon. All column chromatography of ligands was carried out by "flash chromatography"[55] using either silica gel (60–200 mesh) or alumina (80–200 mesh). Fractions from column chromatography were monitored by using Baker-Flex 1B-F TLC plates. Purity of ligands was judged by TLC and ^1H NMR.

Elemental analyses were performed by Galbraith Laboratories, Inc., Knoxville, TN, and/or MicAnal, Tucson, AZ. Infrared spectra were taken on either a Perkin-Elmer 283 or 710B instrument, and ^1H NMR spectra were recorded on a Varian EM 360 60-MHz spectrometer with shifts reported as δ values downfield from an internal standard of Me_4Si. UV/vis/near-IR spectra were recorded on a Cary 14 spectrophotometer as described below. X-band EPR measurements were taken by using a Varian E-4 spectrometer in frozen CH_2Cl_2 solution at 77 K; calibration was effected by using diphenylpicrylhydrazyl (DPPH).

Gas (O_2 and CO) Uptake Measurements. A gas burette system similar to that described by McAuliffe and co-workers[56] or Coleman and Taylor[57] was employed for gas-uptake measurements at constant pressure. This consisted of a 50-mL burette filled with mercury (Hg) attached by a tube at the bottom going to a Hg resevoir and at the upper part of the burette going to a U-tube partially filled with Hg. Both resevoir and "far" end of the U-tube were open to the atmosphere, and the burette and U-tube were enclosed in a large air-jacketed condenser tube. At the top of the burette just above the air-jacket was a three-way stopcock, one opening leading to a vacuum line and the other to the reaction flask. The reaction flask (usually 50 mL with side-arm stopcock(s)) was attached to the burette stopcock with a short length of vacuum hose, and the portion of the reaction flask below the stopcock was immersed in a Dewar flask for maintenance of low temperature. The temperature (usually ca. −80 °C) was controlled and maintained by careful monitoring of a dry ice/acetone mixture or by using a Neslab Instruments cryocool immersion cooler (CC-100II) in a Neslab agitainer bath with methanol as coolant solvent. The temperature was monitored with an Omega Model 651 digital resistance thermometer.

A 50-mL reaction flask with a side arm was charged with the CH_2Cl_2 solvent (~40 mL) and magnetic stirbar under Ar and fitted with a side-arm bent tube, containing a weighed amount of the complex **1**. (The crystalline solid is not very air sensitive and can be handled briefly in air or O_2.) The side arm of this flask was attached to the burette assembly, the reaction flask was immersed into the low-temperature bath, and the solution and system were allowed to equilibrate with 1 atm of O_2 by employing three vacuum/O_2 purges and waiting until a constant volume in the buretie was read while leveling in the U-tube and Hg resevoir (at room temperature). Twisting of the side-arm bent tube dumped the solid sample **1** into the O_2-containing solution, and this was stirred rapidly as the reaction took place. The reaction was monitored (usually for several hours before completion) by the volume change in the burette. The volume of gas was read in the buretie by again adjusting the Hg resevoir height, such that the Hg levels in the two arms of the U-tubes were equalized; the final reading was taken when no further change occured over a 30-min period.

The number of moles of gas taken up was calculated by using the ideal gas law with the room temperature for T and the pressure (barometer) for P. Good reproducibility was possible with this apparatus in spite of the temperature gradient between the burette assembly and reaction flask. The absolute accuracy of the system was checked by using complex II ($Cu:O_2$ = 2:1).[17]

For four runs using ca. 0.5 mmol of the dicopper(I) complex **1** at −80 °C, the $Cu:O_2$ ratio was found to be 2.0 ± 0.1. The uptake of CO at −80 °C by 0.52 g (0.62 mmol) of **1** using the same apparatus was found to be 1.22 mmol or 99% of the amount expected for the formation of **3a** (Cu:CO = 2:2).

Low-Temperature UV–Vis Spectroscopy. Spectra of **1**, **2**, and **3a** were obtained at −80 °C in CH_2Cl_2 by using the Cary 14 spectrophotometer adapted with a light-proof rectangular box fitted to the sample compartment to allow the insertion of a Kontes KM-611772 variable-temperature vis/UV Dewar cell (including cuvette assembly). A stand was constructed to hold the Dewar assembly in a rigid and reproducible way within the sample compartment. Cooling was achieved by inserting a coil of copper tubing into the methanol-filled Dewar through which cold methanol was circulated from an external source (Neslab CC-100II cryocool immersion cooler, in Agitainer A with circulating pump). The copper coil was placed so that it remained above the quartz windows of the Dewar and allowing the cuvette assembly (standard 1-cm cuvette attached to 8-in. glass tubing with stopcock and 14/20 female joint at top) to be inserted through the middle of the coil. The temperature was monitored next to the cuvette by using either the Omega Model 651 resistance thermometer or Model 650 thermocouple thermometer probe. Dry nitrogen was passed through the sample compartment on humid days to prevent fogging of the windows. This apparatus allowed data to be taken down to approximately 330 nm below which the absorption due to the apparatus and/or methanol coolant became too large. The spectrum of the solvent alone in the apparatus was also recorded for each set of runs, and the sample spectra were thus base-line-corrected by digitizing all spectra by hand, taking points every 3–5 nm and regraphing.

Solid samples of **1** were quickly weighed in the air on an analytical balance, transferred to the cuvette assembly, and placed under Ar by vacuum-purge cycling. Carefully purified dichloromethane was directly distilled from CaH_2 into the cuvette assembly, usually by chilling the cuvette while the entire apparatus is at room temperature and under a static vacuum). After placing the cuvette into the Dewar assembly, 10 min was allowed for temperature equilibration and the spectrum recorded. The cuvette assembly was previously calibrated for volume vs. height in the tube, and the height of the solution in the cuvette assembly at low temperature was noted for the purposes of concentration determination.

Oxygenation of the chilled solution of **1** was effected by direct bubbling of dry dioxygen (≥5 min) using a glass tube or syringe needle or by introducing O_2 from a vacuum line and vigorously shaking the solution. The purple peroxide complex **2** was reconverted to **1** by (a) applying a vacuum at low temperature, (b) bringing up a bath of boiling water around the cuvette for a few seconds till the purple color was lost and the color of **1** restored, and (c) recooling the solution and redistilling into the cuvette the exact amount of dichloromethane (up to a previously noted mark on the tube) which had been lost by this procedure. The process could be repeated to effect the "vacuum-cycling" of **1** and **2**.

Coordinated CO ligands in **3a** were removed by the application of a vacuum at room temperature to the CH_2Cl_2 solution to form **1**. Argon was admitted to the cuvette assembly, and the vacuum was applied again and the process repeated for several cycles. Fresh dichloromethane was distilled in to replace that lost, and it was made up to a predetermined volume (mark on a precalibrated cuvette tube assembly). After the spectrum was recorded at −80 °C, complex **2** was produced by admitting O_2. To convert this to **3a**, the solution was saturated with CO by bub-

(55) Still, W. C.; Kahn, M.; Mitra, A. *J. Org. Chem.* **1978**, *43*, 2923–2925.
(56) McAuliffe, C. A.; Al-Khateeb, H. F.; Barratt, D. S.; Briggs, J. C.; Challita, A.; Hosseiny, A.; Little, M. G.; Mackie, A. G.; Minten, K. *J. Chem. Soc., Dalton Trans.* **1983**, 2147–2153.
(57) Coleman, W. M.; Taylor, L. T. *Inorg. Chem.* **1977**, *16*, 1114–1119.

bling it in this gas for 5–10 min and the solution was slowly warmed by removing it from the Dewar and shaking it until the color of **2** was lost. Again, the spectrum of **3a** was recorded at low temperature, and the process was repeated.

Dicopper(I) Complex $[Cu_2(XYL\text{-}O\text{-})]PF_6$ (1). A warm (50 °C) solution of 5.13 g (13.8 mmol) of $[Cu(CH_3CN)_4]PF_6$[58] in 160 mL of MeOH was added to a solution of 3.94 g (6.88 mmol) of XYL-OH[17] and 1.10 g (27.7 mmol) of NaOH in 100 mL of methanol, giving a turbid orange solution. This was filtered, and the volume slowly reduced under vacuum at 0 °C to 50 mL whereupon orange crystals were deposited. The crystals were washed twice with small volumes of cold MeOH and dried under vacuum with a yield of 4.2 g (72%). Anal. Calcd for $C_{36}H_{39}Cu_2F_6N_6OP$: C, 51.24; H, 4.66; N, 9.96. Found: C, 51.44; H, 4.66; N, 9.94. UV–vis (CH_2Cl_2, −80 °C): λ_{max}, nm (ϵ, M^{-1} cm^{-1}) 320 (9100), 385 (10500).

Recently, we have developed a more efficient synthesis of **1**, via the direct chemical reduction of III with 1,2-diphenylhydrazine in the presence of base. As it pertains to other work in progress, the synthetic details of this procedure will be reported elsewhere.[59]

Dicopper(I) Complex $[Cu_2(XYL\text{-}O\text{-})(PPh_3)_2]PF_6\cdot CH_2Cl_2$ (3b). Triphenylphosphine (0.20 g, 0.76 mmol) was added to complex **1** (0.20 g, 0.256 mmol) dissolved in 15 mL of CH_2Cl_2, and the mixture was stirred. Over 30 min the orange solution turned to a faint yellow color whereupon diethylether was added to the cloud point, the solution was filtered, and faintly yellow crystals formed on standing overnight. The supernatant solution was decanted, and the crystals were washed two times with ether and dried under vacuum to yield 0.22 g (82%) of $[Cu_2(XYL\text{-}O\text{-})(PPh_3)_2]PF_6\cdot CH_2Cl_2$ (**3b**). Anal. Calcd for $C_{73}H_{71}Cl_2Cu_2F_6N_6OP_3$: C, 60.33; H, 4.89; N, 5.79. Found: C, 60.23; H, 5.25; N, 5.92.

Reaction of 2 with PPh_3 at −80 °C. Synthesis of $[Cu_2(XYL\text{-}O\text{-})(PPh_3)_2]PF_6\cdot CH_2Cl_2$ (3b). Complex **1** (0.40 g, 0.47 mmol) was dissolved in 25 mL of degassed CH_2Cl_2 under Ar and cooled to −80 °C followed by bubbling of dry O_2 gas through this solution. After 10 min of bubbling, the excess O_2 was pumped off and the intensely purple solution was purged with Ar. Triphenylphosphine (0.30 g, 1.15 mmol) was added under Ar and the solution stirred for 10–15 min. The purple color faded gradually resulting in a faintly yellow solution. This was filtered under Ar and allowed to warm up to room temperature. Degassed Et_2O was added until a cloudy solution was obtained. The solution was filtered again, and upon standing overnight at room temperature, light yellow crystals formed. Filtration, washing with Et_2O, and drying in vacuo afforded 0.67 g (98.5%) of **3b**. Anal. Calcd for $C_{73}H_{71}Cl_2Cu_2F_6N_6OP_3$: C, 60.33; H, 4.89; N, 5.79. Found: C, 60.69; H, 4.99; N, 5.77. NMR (^1H, CD_3CN): δ 2.8 (16 H, br, s), 3.35 (4 H, br, s), 5.43 (2 H, CH_2Cl_2), 6.7–7.7 (45 H, m), 8.12 (4 H, (py-6), d).

Reaction of 2 with PPh_3. Manometric Measurement of the Quantitative Release of O_2. As described above, a 50-mL side-arm flask containing 40 mL of dry degassed CH_2Cl_2 was fitted on top with a ground-glass-jointed Y-adapter to which two Kontes K-218700 storage tubes (bent) were attached; one tube contained triphenylphosphine (0.31 g, 1.18 mmol) and the other had granular microcrystals of complex **1** (0.465 g, 0.55 mmol). The apparatus was attached to the manometer system via the side arm of the 50-mL flask, and the entire apparatus was charged and equilibrated with O_2 to 1-atm pressure (over 2–3 h) with the reaction flask at −80 °C. The tube containing **1** was rotated to empty the contents into the cold dichloromethane whereupon it immediately turned purple as the O_2 pressure in the manometer dropped. Equilibration took ca. 2.5 h, and the volume of O_2 taken up (13.2 mL) corresponded to 0.544 mmol or 98.6% of expected for the formation of complex **2**. At this time, the triphenylphosphine was added into the reaction flask, whereupon within a few minutes 13.0 mL of a gas (O_2) was released (corresponding to 98.5% of the O_2 taken up). Precipitation of the contents of the reaction flask by addition of cold diethyl ether and isolation as described above afforded 0.80 g of $[Cu_2(XYL\text{-}O\text{-})(PPh_3)_2]PF_6\cdot CH_2Cl_2$ (93.0% yield), compound **3b**. Crystals suitable for X-ray analysis were isolated from this preparation by recrystallization from CH_2Cl_2/Et_2O at room temperature.

Test for O_2 Given off from the Reaction of 2 with PPh_3 or CO at −80 °C in CH_2Cl_2. To a 50-mL Schlenk reaction vessel (Ace 7756) with stopcock and two ground glass joints were attached a storage tube containing triphenylphosphine and an attachment to a vacuum/gas line. The stopcock on the vessel was attached via a short length of vacuum hose to a side-arm flask fitted on top with a addition funnel (Kontes K-215200) containing a colorless (O_2 free, Ar purged) alkaline pyrogallol O_2 test solution.[30] In this way, solutions in the reaction vessel could be bubbled with a gas (Ar or CO) and swept into the pyrogallol test solution. A dichloromethane (−80 °C) solution of **2** was prepared in the reaction vessel by bubbling a solution of **1** with O_2 for 10 min, and excess O_2 was pumped off by the application of several vacuum/purge (Ar) cycles. Ar was then allowed to bubble directly through the purple solution of **2** and into the pyrogallol solution for 15 min; no color development or change was observed. While the Ar was bubbling in this fashion, the triphenylphosphine was tipped into the reaction vessel. After 15–30 s, the pyrogallol solution started to turn brown gradually growing darker as the purple color inside the reaction vessel faded, indicating that O_2 is released from **2** upon addition of PPh_3.

In a separate experiment, CO was bubbled through the solution of **2**, but at −80 °C, no color development in the pyrogallol solution was observed over a 30–45-min period, indicating that O_2 is not displaced by CO at this temperature. However, when the purple solution of **2** is slightly warmed (repeated removal from −80 °C bath for 1 min and then recooling) while bubbling with CO, the purple color faded and the pyrogallol test solution turned to the characteristic brown color indicative of exposure to O_2. The CO complex **3a** formed in the reaction vessel could be converted to **1** by the application of vacuum/Ar purging cycles with warming. Rechilling and exposure to dioxygen gives the purple solution of **2**, and CO could then be used again to displace the O_2 as described above.

X-ray Crystallography, Crystallization, Data Collection, and Reduction. Crystals suitable for X-ray diffraction were prepared as described above. Epoxy-covered crystals of compounds **1** and **3b** were mounted on a Nicolet R3m four-circle automated diffractometer with a Mo X-ray source equipped with a highly ordered graphite monochromater (λ(Mo Kα) = 0.71073 Å). Automatic centering and least-squares routines were carried out on 19 reflections for compound **1** and 22 reflections for compound **3b** to obtain the cell dimensions that are given in Table I. A coupled θ(crystal)–2θ(counter) scan mode was employed. The scan length was $(2\theta(K\alpha_1 - 1.0))°$ to $(2\theta(K\alpha_2 + 1.0))°$. Three check reflections were measured every 197 reflections; these exhibited no significant decay during data collection. The program XTAPE of the SHELXTL package[60] was used to process the data for both complexes. A summary of cell parameters, data collection parameters, and refinement results for complexes **1** and **3b** is found in Table I.

Structure Solution and Refinement. The positional parameters of the copper atoms were determined by direct methods for complex **1** and by the Patterson method in the case of complex **3b**. The remaining nonhydrogen atoms were located by subsequent difference Fourier maps and least-square refinements. Atomic scattering factors for neutral atoms were used throughout the analysis. Complex **1** crystallizes in the monoclinic space group $P2_1/n$ with eight molecules per unit cell. There are two crystallographically independent molecules in each asymmetric unit. Compound **3b** crystallizes in the triclinic space group $P\bar{1}$ with $Z = 2$. For **1**, all non-hydrogen atoms were refined anisotropically. For complex **3b**, anisotropic refinement was carried out on copper atoms, phosphorous atoms of the PPh_3 and PF_6^- groups, and the oxygen atom. The remaining atoms were refined isotropically. For complex **3b**, aromatic rings were refined as rigid (fixed) groups. In both cases, the hydrogen atoms were included in the final stages of refinement for the complex cation. The carbon–hydrogen bond distance was set at 0.96 Å, with isotropic thermal parameters 1.2 times those of the bonded carbon atoms. Some disorder is seen for the hexafluorphosphate anions that are present in both compounds. Two fragments of dichloromethane, each with an occupancy factor of 0.5 were located in the final stages of refinement for compound **3b**. Both of the fragments accounted for one molecule of dichloromethane as a solvent of crystallization. For both complexes, data were corrected for the background, attenuator, Lorentz, and polarization effects in the usual fashion.[61] The highest peaks in the final difference map of complex **1** corresponded to half an electron and were found in the region of one of the PF_6^- ions at a distance of 1.6 Å from the P atom. The final R factors and refinement data appear in Table I.

Structure factors, bond lengths, bond angles, anisotropic temperature factors, and hydrogen coordinates and temperature factors are available as supplementary material for compounds **1** (Tables VI–X) and **3b** (Tables XI–XV).

Acknowledgment. We thank the National Institutes of Health for their generous support of this research. We also wish to thank J. E. Pate and E. I. Solomon of Stanford University for helpful

(58) Kubas, G. J. *Inorg. Synth.* **1979**, *19*, 90.
(59) Karlin, K. D., et al., work in progress.

(60) All calculations were performed on a Data general Nova 3 computer with 32K of 16-bit words using local versions of the Nicolet SHELXTL interactive crystallographic software package, as described in: Sheldrick, G. M. *Nicolet SHELXTL Operations Manual*; Nicolet XRD Corp.: Cupertino, CA, 1979.
(61) Hyde, J.; Venkatasubramanian, K.; Zubieta, J. *Inorg. Chem.* **1978**, *17*, 414.

discussions and their contributions relating to spectroscopic studies of the system described.

Note Added in Proof. An EXAFS study of **2** and related relevant compounds reveals that the Cu···Cu distance in this dioxygen complex is 3.31 Å.[41] This finding precludes a μ-1,1-type of peroxo coordination to the dicopper(II) center. The resonance Raman investigation shows that the peroxo ligand is bound in an asymmetric fashion, suggesting either a terminal coordination to a single Cu(II) atom or a μ-1,2 peroxo binding to inequivalent coppers.[28]

Supplementary Material Available: ORTEP diagram of the complete cation of **3b** and listings of bond lengths, bond angles, anisotropic temperature factors, and hydrogen coordinates and temperature factors for **1** (Tables VII-X) and **3b** (Tables XII-XV) (21 pages); listings of structure factors (33 pages). Ordering information is given on any current masthead page.

Effect of a Dipole Moment on the Ionic Strength Dependence of Electron-Transfer Reactions of Cytochrome *c*

J. D. Rush,[†] J. Lan, and W. H. Koppenol*[†]

Contribution from the Department of Chemistry, University of Maryland Baltimore County, Catonsville, Maryland 21228. *Received October 6, 1986*

Abstract: The ionic strength dependence of electron-transfer reactions between metal ion complexes of varying overall charge, $Fe^{II}edta^{2-}$, $Fe^{II}cydta^{2-}$, $Fe^{II}dtpa^{3-}$, $Co(oxalate)_3^{3-}$, and $Ru(NH_3)_6^{2+}$, and horse-heart ferri- and ferrocytochrome *c* was measured. Cytochrome *c* has a large dipole moment ($\sim$300 D) which intersects the protein surface near the presumed site of electron transfer close to the solvent accessible haem edge. The equation derived by Van Leeuwen et al. [*Biochim. Biophys. Acta* **1981**, *635*, 434], which, in addition to net charges, takes into account the dipole moment of a protein, fits the experimental ionic strength dependences very well. The following known parameters were inserted in the equation: net charges of $+7e$ and $+6e$ for ferri- and ferrocytochrome *c*, respectively, an angle of 30° between the dipole vector and the haem plane, and dipole moments of 312 and 300 D for ferri- and ferrocytochrome *c*, respectively.

Studies of reactions of singly modified horse heart cytochromes *c* with small redox agents showed that electron transfer takes place at the solvent accessibile haem edge,[1-4] which forms only 0.6% of the total surface area[5] of the molecule. The distribution of charges on the surface of cytochrome *c* is asymmetric.[6] It guides negatively charged redox agents to a location near the haem edge and increases thereby the number of productive encounters. One would expect the dipole moment to have an effect on the ionic strength dependence of the simple reactions of cytochrome *c* with small, charged, molecules. Currently, there are only two theories which take into account the effect of a dipole moment on the kinetic ionic strength effect. While these theories are in agreement with each other as far as the effect of net charges on the ionic strength dependence is concerned, the equation derived by Koppenol[7] indicates a contribution from the dipole moment to the ionic strength dependence which is approximately twice as large as that predicted by the theory of Van Leeuwen et al.[8] Both theories could be used to estimate the site of electron transfer relative to the dipole axis of a protein molecule if the location of this site were unknown. Neither theory has been applied to kinetic data obtained over a wide range of ionic strengths. We report here on the ionic strength dependences of the reactions of a protein molecule with a known site of interaction, cytochrome *c*, with a variety of small redox agents. Equations which take into account only the net charge of the reactants do not adequately describe the reactions, while the equation derived by Van Leeuwen et al.[8] fits the observed dependences quite well.

Experimental Section

Kinetic experiments were performed either with a Beckmann DU-6 HS spectrophotometer or a Kinetic Instruments, Inc. stopped-flow apparatus equipped with an OLIS optical system and data acquisition system (OLIS 3920). All experiments requiring anaerobic conditions were performed with the stopped-flow apparatus. Ionic strength was maintained with NaCl. The contribution to ionic strength from the buffer (Na,K-phosphate, pH 7.0 ± 0.2) was included. At low salt concentrations (0.1 mM $\leq$ ionic strength $\leq$ 5 mM) the buffer contributed up to 15% to the ionic strength and ca. 5% at higher ionic strengths. pH's were checked at the stopped-flow exhaust port when small buffer concentrations were employed. Experiments were carried out at 25 °C.

Reactions were studied at 550 nm under pseudo-first-order conditions in mediator concentrations. Rate constants were the mean of three runs (generally reproducible to within 5%), and bimolecular rate constants were calculated from three runs over a four-to-eight-fold range of mediator concentrations.

Solutions of horse heart ferricytochrome *c*, Type VI (Sigma), were freshly prepared and degassed with N_2 (99.99%) for a minimum period to prevent denaturation. Ferrocytochrome *c* was prepared by reaction with sodium ascorbate, followed by gel filtration (Sephadex G-15) and elution with deaerated (N_2) 0.2 M phosphate buffer.

Stock solutions of the ferrous edta, dtpa, and cydta complexes were prepared by dissolving $Fe(NH_4)_2(SO_4)_2 \cdot 6H_2O$ in a deaerated (N_2) solution containing 30% excess of ligand. The purity of the synthesized ruthenium(II) hexammine chloride[9] was determined to be 98±% by comparison of its absorption spectrum with literature values[10] [$\lambda_{max}(\epsilon)$ = 275 nm (640 M^{-1} cm^{-1}), 385 nm (40 M^{-1} cm^{-1})]. Solutions of this compound are reported to react slowly with dissolved N_2. Therefore, small amounts of solution were prepared and used within 10 min. Potassium (trisoxalato)cobaltate(III) was prepared by oxidizing a $CoCl_2$-$K_2C_2O_4$ (1:3) solution with lead dioxide and precipitating the green

[†] Address as of June 15th, 1987: Department of Chemistry, Louisiana State University, Baton Rouge, Louisiana 70803.

(1) Butler, J.; Davies, D. M.; Sykes, A. G.; Koppenol, W. H.; Osheroff, N.; Margoliash, E. *J. Am. Chem. Soc.* **1981**, *103*, 469.
(2) Ahmed, A. J.; Miller, F. *J. Biol. Chem.* **1981**, *256*, 1611.
(3) Butler, J.; Koppenol, W. H.; Margoliash, E. *J. Biol. Chem.* **1982**, *257*, 10747.
(4) Armstrong, G. D.; Chambers, J. A.; Sykes, A. G. *J. Chem. Soc., Dalton Trans.* **1986**, 755.
(5) Stellwagen, E. *Nature (London)* **1978**, *275*, 73.
(6) Koppenol, W. H.; Margoliash, E. *J. Biol. Chem.* **1982**, *257*, 4426.
(7) Koppenol, W. H. *Biophys. J.* **1980**, *29*, 493.
(8) van Leeuwen, J. W.; Mofers, F.; Veerman, E. *Biochim. Biophys. Acta* **1981**, *635*, 434.
(9) Lever, F. M.; Powell, A. R. *J. Chem. Soc. A* **1969**, 1477.
(10) Schmidtke, H.-H.; Garthoff, D. *Helv. Chim. Acta* **1966**, *49*, 2039.

0002-7863/87/1509-2679$01.50/0